

# Amplitude representation of Landau-Lifshitz equation and its application to ferromagnetic films.

Gang Li<sup>1\*</sup> and Valery Pokrovsky<sup>1,2</sup>

January 5, 2023

<sup>1</sup>Department of Physics and Astronomy, Texas A&M University, College Station, TX 77843-4242, USA.

<sup>2</sup>Landau Institute for Theoretical Physics of Russian Academy of Sciences, Chernogolovka, 142432, Russian Federation.

\*dgzy03@gmail.com

## 1 Introduction

In 1935 Lev Landau and Evgenii Lifshitz set the foundation of static and dynamics of weakly anisotropic ferromagnets [1, 2]. They formulated the famous Landau-Lifshitz equation (LLE) that regulates the motion of the ferromagnet magnetization in the long-wave low-frequency limit. The purpose of this article is to develop a systematic approach to the solution of the LLE in terms of the magnon wave function  $\psi(\mathbf{r})$  and apply it to physical phenomena in a thin ferromagnetic film.

This problem has a long history. First such approach was proposed by Schlöman in 1959 [3] for a bulk ferromagnet. It was developed and improved by Carl Patton and his coworkers (see references in the review article by Krivosik and Patton [4]). The applications focused on the ferromagnetic resonance (FMR) and the spin momentum transfer, i.e., spin currents.

The theoretical study of ferromagnetic films started also in the the middle of 20-th century by the seminal work of Damon and Eshbach [5]. They have found exact solution of the LLE equation for an infinite ferromagnetic film in which spins interact only through the dipolar forces. In sufficiently thick films the evanescent waves propagating in opposite direction at the two surfaces appear. They create a mechanical torque acting on the film.

Gann [6], De Wames and Wolfram [7], Kalinikos and Slavin [8, 9] extended the Damon-Eshbach theory to a more general situation in which the spins interact also through the exchange forces. An extension of these exact solutions for

the tilted external magnetic field was found by Arias [10]. In the work by the authors, Chen Sun and Thomas Nattermann [11] the solution was extended to the wide range of the film thickness. It enabled us to follow the transition from the magnon spectrum with two symmetric minima in thick films to one-minimum spectra in thin films.

The latter result was inspired by the discovery of the Bose-Einstein condensation of magnons (BECM) at room temperature under permanent pumping of electromagnetic waves made in 2006 by Demokritov *et al*[12]. The BECM was found in the Yttrium Iron Garnet (YIG), a strongly insulating ferrite. For long-wave excitations all spins in the primitive cells move as a whole. It means that in this regime the ferrite is indistinguishable from a ferromagnet.

The amplitude representation (AR) is ideally adjusted to describe the condensation. The condensate amplitudes  $\psi_{\pm}$  are the Fourier components of the coordinate wave functions  $\psi(\mathbf{r})$  at the values of wave vector  $\mathbf{k} = \pm\mathbf{Q}$  corresponding to the two symmetric minima of magnon energy. Since we are mostly interested in the properties of the condensate and its interaction with excited magnons, our focus in the study of the (AR) will be different that in already cited works by Schlöman and Patton. Certainly, some overlapping is unavoidable, but we try to minimize it.

This article has also a purpose to represent the modern state of art for the properties of ferromagnetic films and the pumping-induced BECM in them at room temperature. Thus, it can be considered as a review on basic principles and the recent advances in the field.

## 2 Hamiltonian formulation of the Landau-Lifshitz equation and Amplitude representation.

### 2.1 Poisson brackets for spins, magnetic moments and magnetization in discrete and continuous models.

Let us start with a discrete 3d-model of the ferromagnet, in which all spins  $\mathbf{S}_{\mathbf{r}}$  are located in the centers of cubic cells of volume  $v_0$  labeled by vectors  $\mathbf{r}$ . The Poisson brackets for the components of spins are:

$$\{S_k(\mathbf{r}), S_l(\mathbf{r}')\} = \delta_{\mathbf{r},\mathbf{r}'} \varepsilon_{klm} S_m(\mathbf{r}), \quad (1)$$

where Kronecker symbol  $\delta_{\mathbf{r},\mathbf{r}'}$  is equal to 1 when  $\mathbf{r} = \mathbf{r}'$  and 0 otherwise;  $\varepsilon_{klm}$  is absolutely antisymmetric 3d tensor with  $k, l, m$  independently taking values 1,2,3 or  $x, y, z$  that is equal to +1 if the permutation  $k, l, m$  is even and -1 if it is odd. We use the Einstein convention that the summation must be performed over repeated indices.

The magnetic moment of a primitive cell is

$$\mathcal{M}_k = \gamma S_k, \quad (2)$$

where  $\gamma = \frac{e}{2mc}$  is the classical gyromagnetic ratio. The relation (2) becomes evident if one remembers that a spin projection, for example  $S_z$ , is quantized

in units  $\hbar$ . As a consequence, the magnetic moment projection is quantized in units of the Bohr's magneton  $\mu_B = \frac{e\hbar}{2mc}$ . Eq. (1) implies that the Poisson brackets for the components of the magnetic moments are:

$$\{\mathcal{M}_k(\mathbf{r}), \mathcal{M}_l(\mathbf{r}')\} = \gamma \delta_{\mathbf{r}, \mathbf{r}'} \varepsilon_{klm} \mathcal{M}_m(\mathbf{r}). \quad (3)$$

The magnetization is defined as magnetic moment of unit volume. It is expressed in terms of magnetic moments as  $\mathbf{M}(\mathbf{r}) = \frac{\mathcal{M}(\mathbf{r})}{v_0}$ . Therefore the Poisson brackets for magnetization in the discrete model are:

$$\{M_k(\mathbf{r}), M_l(\mathbf{r}')\} = \frac{\gamma}{v_0} \delta_{\mathbf{r}, \mathbf{r}'} \varepsilon_{klm} M_m(\mathbf{r}). \quad (4)$$

In continuous approximation the ratio  $\frac{\delta_{\mathbf{r}, \mathbf{r}'}}{v_0}$  transits into the Dirac  $\delta$ -function:

$$\lim_{v_0 \rightarrow 0} \frac{\delta_{\mathbf{r}, \mathbf{r}'}}{v_0} = \delta(\mathbf{r} - \mathbf{r}'). \quad (5)$$

To prove this statement let us introduce an arbitrary continuous function  $f(\mathbf{r})$ . Let us consider a sum over the sites of the discrete model:

$$v_0 \sum_{\mathbf{r}'} \frac{\delta_{\mathbf{r}, \mathbf{r}'}}{v_0} f(\mathbf{r}') = f(\mathbf{r}).$$

In continuous limit  $v_0 \sum_{\mathbf{r}'} \rightarrow \int d^3r'$ , which, together with previous equation, proves eq. (5).

Thus, the Poisson brackets for components of magnetization in continuous limit are:

$$\{M_k(\mathbf{r}), M_l(\mathbf{r}')\} = \gamma \delta(\mathbf{r} - \mathbf{r}') \varepsilon_{klm} M_m \quad (6)$$

It is convenient to rewrite these relations explicitly as;

$$\{M_x(\mathbf{r}), M_y(\mathbf{r}')\} = \gamma \delta(\mathbf{r} - \mathbf{r}') M_z(\mathbf{r}) \quad (7)$$

Two other Poisson brackets can be obtained from (7) by the cyclical permutation of the indices  $x, y$  and  $z$ . For further applications it is useful to introduce complex transverse magnetizations:

$$M_{\pm}(\mathbf{r}) = M_x(\mathbf{r}) \pm i M_y(\mathbf{r}) \quad (8)$$

For them eq. (7) implies the following Poisson brackets:

$$\begin{aligned} \{M_+(\mathbf{r}), M_-(\mathbf{r}')\} &= -2i\gamma \delta(\mathbf{r} - \mathbf{r}') M_z(\mathbf{r}) \\ \{M_{\pm}(\mathbf{r}), M_z(\mathbf{r}')\} &= \pm i\gamma \delta(\mathbf{r} - \mathbf{r}') M_{\pm}(\mathbf{r}) \end{aligned} \quad (9)$$

## 2.2 Amplitude representation and Poisson brackets for the magnon wave function.

Let the spontaneous magnetization and external magnetic field be directed along  $z$ -axis, perpendicular to its direction in the plane of film be  $y$  and direction

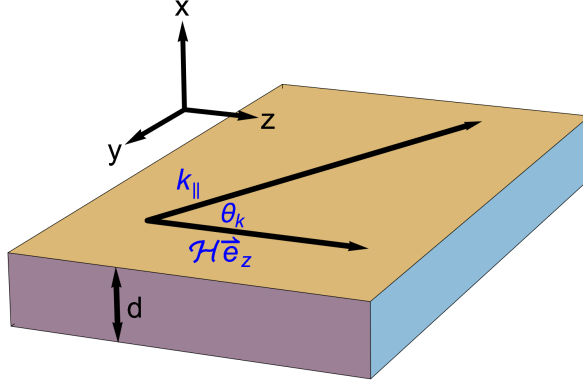


Figure 1: The coordinate system for a ferromagnetic film of thickness  $d$ :  $z$ -axis is chosen along the common direction of the magnetic field and static magnetization,  $x$ -axis is perpendicular to the film,  $\theta_k$  is the angle between the magnon wave vector and magnetic field.

perpendicular to the film  $x$  as shown in Fig. 1. The wave function of magnons  $\psi(\mathbf{r})$  is determined by the magnon classical Holstein-Primakoff transformation:

$$\begin{aligned} M_+(\mathbf{r}) &= \sqrt{\mu_B} \psi(\mathbf{r}) \sqrt{2M - \mu_B \psi^*(\mathbf{r}) \psi(\mathbf{r})} \\ M_-(\mathbf{r}) &= \sqrt{\mu_B} \psi^*(\mathbf{r}) \sqrt{2M - \mu_B \psi^*(\mathbf{r}) \psi(\mathbf{r})} , \\ M_z &= M - \mu_B \psi^*(\mathbf{r}) \psi(\mathbf{r}) \end{aligned} \quad (10)$$

where  $M$  is the magnitude of magnetization vector that is assumed to be constant. The third equation (10) shows that the physical meaning of the square of modulus  $\psi^*(\mathbf{r}) \psi(\mathbf{r})$  is the density of magnons  $n(\mathbf{r})$ . Note that the order of factors in eqs. (10) is not important. The second useful remark is that  $\sqrt{2M - \mu_B \psi^*(\mathbf{r}) \psi(\mathbf{r})} = \sqrt{M + M_z}$ .

The equations (9) are compatible with the amplitude representation (10) if and only if the wave functions satisfy the following permutation relations:

$$\begin{aligned} \{\psi(\mathbf{r}), \psi^*(\mathbf{r}')\} &= -\frac{i}{\hbar} \delta(\mathbf{r} - \mathbf{r}') \\ \{\psi(\mathbf{r}), \psi(\mathbf{r}')\} &= \{\psi^*(\mathbf{r}), \psi^*(\mathbf{r}')\} = 0 \end{aligned} \quad (11)$$

Let us prove this theorem for the second equation (9). We will use the algebraic identity valid for any algebra of operators with defined operations of addition and non-commutative multiplication:

$$\{AB, C\} = A\{B, C\}C + \{A, C\}B \quad (12)$$

Employing this rule and the third equation (10), we find:

$$\begin{aligned} \{M_+, M_z\} &= \sqrt{\mu_B} \{ \psi(\mathbf{r}) \sqrt{M + M_z(\mathbf{r})}, M_z(\mathbf{r}') \} = \\ \sqrt{\mu_B (M + M_z(\mathbf{r}))} \{ \psi(\mathbf{r}), M_z(\mathbf{r}') \} &= -\sqrt{\mu_B^3 (M + M_z(\mathbf{r}))} \{ \psi(\mathbf{r}), \psi^*(\mathbf{r}') \psi(\mathbf{r}') \} \end{aligned}$$

Applying again the identity (12) and assuming that  $\{ \psi(\mathbf{r}), \psi(\mathbf{r}') \} = 0$ , we arrive at relation

$$\{M_+, M_z\} = -\sqrt{\mu_B^3 (M + M_z(\mathbf{r}))} \psi(\mathbf{r}') \{ \psi(\mathbf{r}), \psi^*(\mathbf{r}') \}$$

The right-hand side of this equation must be equal to  $i\gamma\delta(\mathbf{r} - \mathbf{r}') M_+(\mathbf{r})$  according to the second equation (9). The necessary and sufficient requirement to satisfy this condition is given by eqs. (11). The validity of the first equation (9) can be checked by a similar calculation.

### 2.3 Landau-Lifshitz Hamiltonian.

The Landau-Lifshitz Hamiltonian  $H_{LL}$  for our problem contains several parts: the exchange interaction  $H_{ex}$ , the dipolar interaction  $H_{dip}$  and the Zeeman interaction  $H_Z$ . It can also may contain the anisotropy (spin-orbit) energy  $H_{an}$ . First we write them in terms of magnetization:

$$H_{LL} = H_{ex} + H_{dip} + H_Z + H_{an}, \quad (13)$$

where:

$$H_{ex} = \frac{D}{2} \int (\nabla \mathbf{M})^2 dV \equiv \frac{D}{2} \int \partial_i M_j \partial_i M_j dV; \quad (14)$$

$$H_Z = -\mathcal{H} \int M_z dV \quad (15)$$

$$H_{dip} = \frac{1}{2} \iint (\mathbf{M} \nabla) (\mathbf{M}' \nabla') \frac{1}{|\mathbf{r} - \mathbf{r}'|} dV dV', \quad (16)$$

In eq. (16) we omitted for brevity the arguments in functions denoting  $\mathbf{M} = \mathbf{M}(\mathbf{r})$ ;  $\mathbf{M}' = \mathbf{M}(\mathbf{r}')$ ;  $\nabla = \nabla_{\mathbf{r}}$ ;  $\nabla' = \nabla_{\mathbf{r}'}$ . When employing the amplitude representation for the components of magnetization (10), we similarly use abbreviations  $\psi \equiv \psi(\mathbf{r})$ ,  $\psi' \equiv \psi(\mathbf{r}')$  and  $\partial_{\pm} \equiv \partial_x \pm i\partial_y$ ,  $\partial'_{\pm} \equiv \partial_{x'} \pm i\partial_{y'}$ . The exchange constant  $D$  determines the exchange length  $\ell = \sqrt{D}$  that separates the length range, in which the dipolar interaction dominates  $l \gg \ell$ , from the range  $l \ll \ell$  where exchange interaction dominates.

The LL equation assumes that the magnitude of the magnetization vector rapidly relaxes to its equilibrium value. Thus, the LL equation describes the relatively slow motion of the vector  $\mathbf{M}(\mathbf{r}, t)$  on the sphere. The slowness of this motion in space and time is controlled by two small parameters  $a/\lambda$  and  $\omega\tau_M$ , where  $a$  is the lattice constant,  $\lambda$  is the wave-length or another characteristic length of the magnetization motion,  $\omega$  is its characteristic frequency and  $\tau_M$  is the relaxation time of the magnetization magnitude. All magnetic phenomena in this limit are dominantly classical since the number of magnons in the volume

with the linear size of the order of  $\lambda$  is large and the change of this number by 1 produces negligibly small change of magnetization.

In terms of amplitudes the three parts of the Hamiltonian given by equations (14,15,16) are

$$H_{ex} = \frac{\mu_B^2 \ell^2}{2} \int (\nabla |\psi|^2)^2 dV + \frac{\mu_B \ell^2}{2} \int \left| \nabla \left( \psi \sqrt{2M - \mu_B |\psi|^2} \right) \right|^2 dV \quad (17)$$

$$H_z = \mu_B \mathcal{H} \int |\psi|^2 dV \quad (18)$$

$$H_{dip} = \frac{1}{2} \iint \hat{\Omega}(\mathbf{r}) \hat{\Omega}(\mathbf{r}') \frac{dV dV'}{|\mathbf{r} - \mathbf{r}'|}, \quad (19)$$

where

$$\hat{\Omega}(\mathbf{r}) = \left( M - \mu_B |\psi|^2 \right) \partial_z + \frac{\sqrt{\mu_B (2M - \mu_B |\psi|^2)}}{2} (\psi \partial_- + \psi^* \partial_+) \quad (20)$$

### 3 Spectrum and wave functions of magnons.

In this section we consider the approximation of free magnons and find their spectrum and wave function. For that purpose it is necessary to separate the part of the total Hamiltonian quadratic in amplitudes  $\psi, \psi^*$  and diagonalize it.

#### 3.1 Quadratic part of the Hamiltonian.

The Zeeman part of the Hamiltonian  $H_Z$  given by eq. (18) is naturally quadratic. The quadratic parts of the exchange and dipolar Hamiltonians are:

$$H_{ex}^{(2)} = \mu_B M \ell^2 \int |\nabla \psi|^2 dV \quad (21)$$

$$H_{dip}^{(2)} = \frac{\mu_B M}{4} \iint (\psi \partial_- + \psi^* \partial_+) (\psi' \partial'_- + \psi'^* \partial'_+) \frac{1}{|\mathbf{r} - \mathbf{r}'|} dV dV' \quad (22)$$

Note that quadratic parts of the exchange Hamiltonian is local in space and it conserves the total number of magnons  $N = \int |\psi|^2 dV$ , whereas the quadratic part of dipolar Hamiltonian is non-local and it violates the conservation of the magnon number. All three parts of the quadratic Hamiltonian are invariant with respect to any translation in the film plane. Therefore, it is natural to describe the motion in plane as a superposition of running plane waves. In other words, the problem must be partly diagonalized by the Fourier-transformation:

$$\psi(\mathbf{r}) = \frac{1}{\sqrt{A}} \sum_{\mathbf{q}} \chi_{\mathbf{q}}(x) e^{i\mathbf{q}\mathbf{r}}, \quad (23)$$

where  $\mathbf{q} = iq_y \hat{y} + iq_z \hat{z}$  is the in-plane wave vector; the Fourier-coefficients  $\chi_{\mathbf{q}}(x)$  depend on the transverse-to-plane coordinate  $x$ ;  $A$  is the area of any film cross-section parallel to its surfaces. The inverse Fourier transformation gives the amplitude of a magnon with the wave vector  $\mathbf{q}$  in a general state with the wave function  $\psi(\mathbf{r})$ :

$$\chi_{\mathbf{q}}(x) = \frac{1}{\sqrt{A}} \iint \psi(\mathbf{r}) e^{i\mathbf{q}\mathbf{r}} dydz \quad (24)$$

Employing the Poisson brackets for  $\psi(\mathbf{r})$  eq. (11), the Poisson brackets for the amplitudes  $\chi_{\mathbf{q}}(x)$  are:

$$\{\chi_{\mathbf{q}}(x), \chi_{\mathbf{q}'}^*(x')\} = -\frac{i}{\hbar} \delta_{\mathbf{q}, \mathbf{q}'} \delta(x - x'). \quad (25)$$

In terms of the variables  $\chi_{\mathbf{q}}(x)$  the three parts of the Hamiltonian are:

$$H_{ex}^{(2)} = \mu_B M \ell^2 \sum_{\mathbf{q}} \int_{-d/2}^{d/2} \left( \left| \frac{d\chi_{\mathbf{q}}(x)}{dx} \right|^2 + \mathbf{q}^2 |\chi_{\mathbf{q}}(x)|^2 \right) dx \quad (26)$$

$$H_Z^{(2)} = \mu_B \mathcal{H} \sum_{\mathbf{q}} \int_{-d/2}^{d/2} |\chi_{\mathbf{q}}(x)|^2 dx \quad (27)$$

$$H_{dip}^{(2)} = \pi \mu_B M \sum_{\mathbf{q}} \iint_{-d/2}^{d/2} [\chi_{\mathbf{q}}(d_x - q_y) + \chi_{-\mathbf{q}}^*(d_x + q_y)] \times [\chi_{-\mathbf{q}}'(d_{x'} + q_y) + \chi_{\mathbf{q}}'^*(d_{x'} - q_y)] G_q(x - x'), \quad (28)$$

where we omitted for brevity the arguments  $x$  and  $x'$  writing  $\chi_{\mathbf{q}}$  instead of  $\chi_{\mathbf{q}}(x)$  and  $\chi_{\mathbf{q}}'$  instead of  $\chi_{\mathbf{q}}(x')$  and employed the abbreviation  $d_x \equiv \frac{d}{dx}$ . The symbol  $G_q(x)$  stays for for the Green function of the 1d Helmholtz equation:

$$G_q(x) = \frac{e^{-q|x|}}{2q} \quad (29)$$

It obeys the 1d Helmholtz equation with a point source at origin:

$$(d_x^2 - q^2) G_q(x) = -\delta(x). \quad (30)$$

### 3.2 Bogoliubov transformation.

The exchange and Zeeman parts of the quadratic Hamiltonian are diagonal in the variables  $\chi_{\mathbf{q}}(x)$ , but the dipolar part mixes  $\chi_{\mathbf{q}}(x)$  with  $\chi_{-\mathbf{q}}^*(x)$ . To diagonalize the total quadratic Hamiltonian we apply the extended Bogoliubov transformation introducing for each  $\mathbf{q}$  an infinite series of variables  $\eta_{\mathbf{q}n}$  associated with  $\chi_{\mathbf{q}}(x)$  and  $\chi_{-\mathbf{q}}^*(x)$  by a linear transformation:

$$\eta_{\mathbf{q}n} = \int_{-d/2}^{d/2} [u_{\mathbf{q}n}(x) \chi_{\mathbf{q}}(x) + v_{\mathbf{q}n}(x) \chi_{-\mathbf{q}}^*(x)] dx. \quad (31)$$

To be canonical this transformation must produce correct Poisson brackets for variables  $\eta_{\mathbf{q}n}$ :

$$\{\eta_{\mathbf{q}n}, \eta_{\mathbf{q}'n'}^*\} = -\frac{i}{\hbar} \delta_{\mathbf{q}, \mathbf{q}'} \delta_{n, n'} \quad (32)$$

This requirement is equivalent to the condition of canonical transformation in classical mechanics [13] or unitary transformation in quantum mechanics. Therefore we will also use the word "unitarity" or "unitary" as equivalent to "canonical". The requirement (32) together with the Bogoliubov transformation (31) and Poisson brackets for  $\chi_{\mathbf{q}}(x)$  (25) implies a series of constraints:

$$\int_{-d/2}^{d/2} [u_{\mathbf{q}n}(x) u_{\mathbf{q}'n'}^*(x) - v_{\mathbf{q}n}(x) v_{\mathbf{q}'n'}^*(x)] dx = \delta_{n, n'} \quad (33)$$

The inverse Bogoliubov transformation determines  $\chi_{\mathbf{q}}(x)$  as a linear combination of  $\eta_{\mathbf{q}n}$ :

$$\chi_{\mathbf{q}}(x) = \sum_n [U_{\mathbf{q}n}(x) \eta_{\mathbf{q}n} + V_{\mathbf{q}n}(x) \eta_{-\mathbf{q}n}^*] \quad (34)$$

Replacing the amplitudes  $\eta_{\mathbf{q}n}, \eta_{-\mathbf{q}n}^*$  in eq. (34) by their Bogoliubov representation (31), we arrive at equations relating direct and inverse Bogolyubov transformations:

$$\begin{aligned} \sum_n [U_{\mathbf{q}n}(x) u_{\mathbf{q}n}(x') + V_{\mathbf{q}n}(x) v_{-\mathbf{q}n}^*(x')] &= \delta(x - x') \\ \sum_n [U_{\mathbf{q}n}(x) v_{\mathbf{q}n}(x') + V_{\mathbf{q}n}(x) u_{-\mathbf{q}n}^*(x')] &= 0 \end{aligned} \quad (35)$$

On the other hand, the unitarity of the inverse Bogoliubov transformation requires

$$\sum_n [U_{\mathbf{q}n}(x) U_{\mathbf{q}n}^*(x') - V_{\mathbf{q}n}(x) V_{\mathbf{q}n}^*(x')] = \delta(x - x') \quad (36)$$

Comparing this equation with the first eq. (29), we arrive at conclusion that  $U_{\mathbf{q}n}(x) = u_{\mathbf{q}n}^*(x)$  and  $V_{\mathbf{q}n}(x) = -v_{-\mathbf{q}n}(x)$ . Thus, the inverse Bogolyubov transformation can be rewritten as

$$\chi_{\mathbf{q}}(x) = \sum_n [u_{\mathbf{q}n}^*(x) \eta_{\mathbf{q}n} - v_{-\mathbf{q}n}(x) \eta_{-\mathbf{q}n}^*] \quad (37)$$

In addition from the  $U - V$  unitarity condition (36) we find the dual unitarity condition in terms of the initial Bogolyubov coefficients:

$$\sum_n [u_{\mathbf{q}n}^*(x) u_{\mathbf{q}n}(x') - v_{-\mathbf{q}n}(x) v_{-\mathbf{q}n}^*(x')] = \delta(x - x') \quad (38)$$

### 3.3 The wave functions and spectrum of magnons.

#### 3.3.1 Spectrum of magnons.

The magnon amplitudes must satisfy the stationary Schrödinger equation whose classical analogue is

$$\{H^{(2)}, \eta_{\mathbf{q}, n}\} = -i\omega_{\mathbf{q}, n} \eta_{\mathbf{q}, n}. \quad (39)$$



The Poisson brackets of the quadratic Hamiltonian and the vector of amplitudes is a linear anti-Hermitian operator acting on this vector. Thus, the vector of amplitudes  $\eta_{\mathbf{q},n}$  is the eigenvector and the frequency of a magnon is the corresponding eigenvalue of the Hermitian operator  $i\{H^{(2)},\}$ . In this subsection we express these equations in terms of the Bogoliubov coefficients. Their solutions in some limiting cases will be found in the next subsection.

In order to write the left part of eq. (39) explicitly, we employ eqs. (26,27,28) for the three parts of the quadratic Hamiltonian, equation (32) for the Poisson brackets of the two amplitude vectors and the Bogoliubov transformation (37) from the amplitudes  $\chi_{\mathbf{q},n}$  to magnon amplitudes  $\eta_{\mathbf{q},n}$ . In resulting equations we omit for brevity the subscripts  $\mathbf{q}$  and  $n$  since they are invariant under the Bogoliubov transformation. Thus, equations (39) can be rewritten as:

$$\begin{aligned} [\omega + \gamma(\mathcal{H} + M\ell^2(\mathbf{q}^2 - d_x^2))] u &= -2\pi\gamma M \left[ (q_y^2 - d_x^2) \zeta_u + (q_y - d_x)^2 \zeta_v \right]; \\ [\omega - \gamma(\mathcal{H} + M\ell^2(\mathbf{q}^2 - d_x^2))] v &= 2\pi\gamma M \left[ (q_y^2 - d_x^2) \zeta_v + (q_y + d_x)^2 \zeta_u \right], \end{aligned} \quad (40)$$

where we denoted  $\gamma = |e|/(2mc)$  is the classical gyromagnetic constant and

$$\zeta_{u,v}(x) = \int_{-d/2}^{d/2} G(x-x') \begin{pmatrix} u(x') \\ v(x') \end{pmatrix} dx'. \quad (41)$$

The physical meaning of the integral terms in the r.-h. side of eqs. (40) is the magnetic field  $\mathbf{h}$  generated by magnon magnetization  $\mathbf{m}$ . The magnetic field can be expressed in terms of magnetostatic potential  $\phi$  as  $\mathbf{h} = -\nabla\phi$ . If it is generated by the magnetization  $\mathbf{m}(\mathbf{r})$ , then

$$\phi(\mathbf{r}) = -\nabla \cdot \int \mathbf{m}(\mathbf{r}') |\mathbf{r} - \mathbf{r}'|^{-1} d^3x' \quad (42)$$

The coefficients  $u$  and  $v$  should be identified with the  $x$ - and  $y$ -components of magnetization, the operators  $\pm iq_y - d_x$  with the complex presentation of gradient and divergence. Then equation (41) is equivalent to (42) integrated over  $y$  and  $z$ .

The reference (40) is a system of two integral-differential equations. However, they can be transformed in the purely differential linear equations by employing operator  $q^2 - d_x^2$  (Laplacian) to both sides of equations (40) and employing eq. (30) to eliminate the Green function  $G(x-x')$ . The application of this operator to  $\zeta_{u,v}(x)$  transforms these integrals into  $u(x)$  and  $v(x)$ , respectively.

Thus, we obtain a system ordinary linear differential equations of the fourth order:

$$\begin{aligned} & [\omega + \gamma(\mathcal{H} + M\ell^2(q^2 - d_x^2))] (q^2 - d_x^2) u \\ &= -2\pi\gamma M \left[ (q_y^2 - d_x^2) u + (q_y - d_x)^2 v \right]; \\ & [\omega - \gamma(\mathcal{H} + M\ell^2(q^2 - d_x^2))] (q^2 - d_x^2) v \\ &= 2\pi\gamma M \left[ (q_y^2 - d_x^2) v + (q_y + d_x)^2 u \right]. \end{aligned} \quad (43)$$

Their solutions must be a superposition of exponents  $e^{i\kappa x}$  with  $\kappa$  being a root of the secular polynomial. To find this polynomial, it is convenient to introduce the vector  $\mathbf{k}$  with the components  $k_x = |\kappa|$ ,  $k_{y,z} = q_{y,z}$  whose square if magnitude is  $k^2 = q^2 + \kappa^2$ . Let us define a simplest solution of the system (43) is:

$$u(x) = u_0 e^{i\kappa x}; v(x) = v_0 e^{i\kappa x} \quad (44)$$

Substituting this solution into eq.(43), we obtain a system of two linear homogeneous equations for  $u_0, v_0$ . The condition of its solvability is the nullification of their determinant (secular equation):

$$\omega^2 k^2 = \gamma^2 (\mathcal{H} + M\ell^2 k^2) \times [(\mathcal{H} + M\ell^2 k^2) k^2 + 4\pi M (k^2 - k_z^2)] \quad (45)$$

This equation can be interpreted as dispersion relation for magnons:

$$\omega = \gamma \sqrt{(\mathcal{H} + M\ell^2 k^2) \left[ \mathcal{H} + M\ell^2 k^2 + \frac{4\pi M (k_x^2 + k_y^2)}{k^2} \right]} \quad (46)$$

It is valid if  $a/\lambda = ka/(2\pi) \ll 1$ . At room temperature the thermal wavelength  $\lambda = \hbar/\sqrt{2mk_B T}$ . For effective mass of magnon for YIG of the order of magnitude  $m \approx 3m_e$ ,  $\lambda$  is about  $0.7nm$ , whereas the lattice constant  $a = 1.2nm$ . Therefore, eq. (46) is invalid for thermal magnons. The calculation of the magnon spectrum at high energies for YIG were given in the seminal article by Kolokolov, L'vov and Cherepanov [14].

### 3.3.2 Bulk and evanescent waves.

At fixed parameters  $\ell, M, \mathcal{H}, k_z = q_z$  and frequency  $\omega$ , eq. (45) is a cubic equation for the variable  $k^2$ . Note that its coefficients do not depend not only on the film thickness  $d$  but also on the value  $k_y$ . Inspection of the coefficients of the cubic equation shows that the product of three roots is positive, whereas their sum is negative. Therefore, there are two opportunities: i) one roots  $k^2$  is positive and two others are negative or ii) one root is positive and two others are complex conjugated with negative real part. Sonin proved [15] that in thick films  $d \gg \ell$  and for  $kl \ll 1$ , the opportunity i) is realized. Gang. Li *et al.* [11] proved that the opportunity ii) leads to negative  $\omega^2$  and therefore is forbidden.

For thick films  $d \gg \ell$  and  $k_z \ll 1/\ell$  and  $\omega^2 < \gamma^2 \mathcal{H} (\mathcal{H} + 4\pi M)$ , the positive root  $k_1^2$  can be found approximately. In this case it is possible to retain in eq. (45) only terms linear in  $k^2$  and independent on  $k^2$  and neglect the terms quadratic and cubic in  $k^2$ . The result is:

$$k_1^2 = k_z^2 \frac{4\pi\gamma^2 \mathcal{H} M}{\gamma^2 \mathcal{H} (\mathcal{H} + 4\pi M) - \omega^2} \quad (47)$$

Two others negative solutions  $k^2 = -\mathfrak{k}_{1,2}^2$  are determined by equation:

$$\mathfrak{k}_{1,2}^2 = \left( 2\pi + \frac{\mathcal{H}}{M} \pm \sqrt{4\pi^2 + \frac{\omega^2}{\gamma^2 M^2}} \right) \ell^{-2} \quad (48)$$

When frequency approaches the ferromagnetic resonance value  $\omega_{FR} = \gamma\sqrt{\mathcal{H}(\mathcal{H} + 4\pi M)}$  to the distance  $\omega_{FR} - \omega \lesssim \frac{k_z^2 \ell^2}{\sqrt{1 + \frac{4\pi\mathcal{H}}{M}}} 2\pi\gamma M$ , the inequality  $k_1 \ell \ll 1$  becomes invalid and instead of quadratic the cubic equation must be solved. At large frequency  $\omega \gg \omega_{FR}$ , the exchange energy dominates and  $\omega \approx \gamma M \ell^2 k^2$ . It corresponds to the region of large wave vectors  $k\ell \gg 1$ . For thick films  $d \gg \ell$ , the four wave functions of the type  $\chi_{\mathbf{q}}(x) \propto \exp[-\mathfrak{k}_{1,2}(\frac{d}{2} \pm x)]$  correspond to the four evanescent waves localized in a layer of the depth  $\sim \ell$  near the surfaces of the film  $x = \pm d/2$ .

### 3.4 Self-consistency.

We proved that any propagating in-plane excitation is a superposition of several transverse modes. The transverse modes may be either superposition of  $\cos k_x x$  and  $\sin k_x x$  or the evanescent waves. However, the inverse statement that any such superposition is a solution of the initial equations of motion is wrong. This happens because the initial equations of motion were integral-differential. The system of ordinary differential equations was obtained from them by application of additional differential operators. This operation introduces additional solutions of resulting system of equations that are not solutions of the initial problem. Below we derive the selection rules that separate only solutions of the initial integral-differential equations (40,41).

Equations for the Bogoliubov transformation functions (40,41) permit real solution. Therefore the Bogoliubov functions can be searched in the form:

$$u_{\mathbf{q},n}(x) = a_n \cos k_x x + b_n \sin k_x x + \sum_{m=1,2} \left( A_{nm} \frac{\cosh \mathfrak{k}_m x}{\cosh \mathfrak{k}_m d/2} + B_{nm} \frac{\sinh \mathfrak{k}_m x}{\sinh \mathfrak{k}_m d/2} \right); \quad (49)$$

$$v_{\mathbf{q},n}(x) = c_n \cos k_x x + d_n \sin k_x x + \sum_{m=1,2} \left( C_{nm} \frac{\cosh \mathfrak{k}_m x}{\cosh \mathfrak{k}_m d/2} + D_{nm} \frac{\sinh \mathfrak{k}_m x}{\sinh \mathfrak{k}_m d/2} \right), \quad (50)$$

where all coefficients  $a_n, b_n, A_{nm}, B_{nm}, c_n, d_n, C_{nm}, D_{nm}$  are real numbers. In further calculations we omit the subscripts  $n$  and  $\mathbf{q}$  since they are fixed. All evanescent waves exponentially decrease far from boundaries on the scale  $\sim \ell$  as  $\exp[-\mathfrak{k}_m |\frac{d}{2} \pm x|]$ .

Substitution of expressions (49,50) to the integral-differential equations (40,41) leads to appearance of exponential functions that do not belong to the 6 exponents permitted by the secular equation (45). They are produced by the integrals (41). Their explicit calculation can be reduced to the four basic integrals:

$$I_c(x) \equiv \int_{-d/2}^{d/2} \frac{e^{-q|x-x'|}}{2q} \cos k_x x' dx' = \frac{\cos k_x x}{k^2} - \frac{e^{-qd/2}}{qk^2} \cosh qx f_1; \quad (51)$$

$$I_s(x) \equiv \int_{-d/2}^{d/2} \frac{e^{-q|x-x'|}}{2q} \sin k_x x' dx' = \frac{\sin k_x x}{k^2} - \frac{e^{-qd/2}}{qk^2} \sinh qx f_2; \quad (52)$$

$$\begin{aligned}
J_{cm}(x) &\equiv \int_{-d/2}^{d/2} \frac{e^{-q|x-x'|}}{2q} \cosh \mathfrak{k}_m x' dx' \\
&= \frac{\cosh \mathfrak{k}_m x}{q^2 - \mathfrak{k}_m^2} - \frac{e^{-qd/2}}{q(q^2 - \mathfrak{k}_m^2)} \cosh qx g_{1m};
\end{aligned} \tag{53}$$

$$\begin{aligned}
J_{sm}(x) &\equiv \int_{-d/2}^{d/2} \frac{e^{-q|x-x'|}}{2q} \sinh \mathfrak{k}_m x' dx' \\
&= \frac{\sinh \mathfrak{k}_m x}{q^2 - \mathfrak{k}_m^2} - \frac{e^{-qd/2}}{q(q^2 - \mathfrak{k}_m^2)} \sinh qx g_{2m},
\end{aligned} \tag{54}$$

where the notations  $f_{1,2}$ ,  $g_{1,2}$  are used for the following functions:

$$f_1 = q \cos \frac{k_x d}{2} - k_x \sin \frac{k_x d}{2}; \tag{55}$$

$$f_2 = q \sin \frac{k_x d}{2} + k_x \cos \frac{k_x d}{2}; \tag{56}$$

$$g_{1m} = q \cosh \frac{\mathfrak{k}_m d}{2} + \mathfrak{k}_m \sinh \frac{\mathfrak{k}_m d}{2}; \tag{57}$$

$$g_{2m} = q \sinh \frac{\mathfrak{k}_m d}{2} + \mathfrak{k}_m \cosh \frac{\mathfrak{k}_m d}{2}. \tag{58}$$

Employing these results, it is possible to calculate  $\zeta_u(x)$  and  $\zeta_v(x)$  defined by eq. (41):

$$\zeta_u(x) = aI_c + bI_s + \sum_{m=1}^2 \left( \frac{A_m J_{cm}}{\cosh \frac{\mathfrak{k}_m d}{2}} + \frac{B_m J_{sm}}{\sinh \frac{\mathfrak{k}_m d}{2}} \right); \tag{59}$$

$$\zeta_v(x) = cI_c + dI_s + \sum_{m=1}^2 \left( \frac{C_m J_{cm}}{\cosh \frac{\mathfrak{k}_m d}{2}} + \frac{D_m J_{sm}}{\sinh \frac{\mathfrak{k}_m d}{2}} \right). \tag{60}$$

The terms with  $I_c$  and  $I_s$  in these equations contain the functions  $\cosh qx$  and  $\sinh qx$  or equivalently  $\exp(\pm qx)$ . The wave vector  $k = q$  does not satisfy the secular equation (45). Therefore, they should vanish in the r.-h. side of eqs. (40). These requirements represent four constraints onto 12 coefficients  $a, b, c, d, A_1, B_1, C_1, D_1, A_2, B_2, C_2, D_2$  [11]. Neglecting evanescent waves in the integrals, we obtain 4 equations for 4 coefficients  $a, b, c, d$  at ‘‘bulk’’ waves:

$$\begin{aligned}
(q_y^2 - q^2) a f_1 &+ (q_y^2 + q^2) c f_1 &+ 2q_y q d f_2 &= 0 \\
(q_y^2 - q^2) b f_2 &+ 2q_y q c f_1 &+ (q_y^2 + q^2) d f_2 &= 0 \\
(q_y^2 + q^2) a f_1 &- 2q_y q b f_2 &+ (q_y^2 - q^2) c f_1 &= 0 \\
-2q_y q a f_1 &+ (q_y^2 + q^2) b f_2 &+ (q_y^2 - q^2) d f_2 &= 0
\end{aligned} \tag{61}$$

The determinant of this system is identically zero. Thus, this system does not determine quantization of  $k_x$ . A simple reason why any  $4 \times 4$  minor of the  $4 \times 24$  matrix formed by coefficients at  $e^{\pm qx}$  in each of the mentioned above twelve coefficients has zero determinant is that all of them obey an inhomogeneous Helmholtz equation, for example,

$$\frac{d^2 I_c}{dx^2} - q^2 I_c = \cos(k_x x); \quad \frac{d^2 J_{cm}}{dx^2} - q^2 J_{cm} = \cosh(k_x x). \tag{62}$$

Since the solutions of such equations can include any linear combination of  $e^{\pm qx}$ , the condition of zero coefficients at these function cannot put any restriction of the  $4 \times 24$  matrix. It means that any its  $4 \times 4$  minor has zero determinant.

The self-consistency equations are equivalent to the MBC, but they simplify calculations.

### 3.5 Boundary conditions and the quantization of transverse modes.

#### 3.5.1 Spin boundary conditions.

There are two kinds of boundary conditions: magnetostatic (MBC) associated with the variation of the magnetic field and induction near the boundary and the spin boundary conditions (SBC) associated with variation of spin (magnetization) at the boundary. The MBC requires continuity of tangential component of magnetic field  $\mathbf{h}$  and the normal component of the induction  $\mathbf{b} = \mathbf{h} + 4\pi\mathbf{m}$  at two surfaces  $x = \pm d/2$  of the film. The MBC are satisfied automatically if the magnetic potential is related to the magnetization by the equation (42). Therefore, only the SBC must be taken into account.

Let us consider the simplest possibility that spins on the surfaces are free. The variation of the exchange energy (14) gives the surface term:

$$\begin{aligned} \delta H_{ex} = \ell^2 \int_{-d/2}^{d/2} dx \iint_{-\infty}^{\infty} dydz \partial_i \delta m_\alpha \cdot \partial_i m_\alpha = \\ \ell^2 \iint_{-\infty}^{\infty} dydz \delta m_\alpha \partial_x m_\alpha \Big|_{-d/2}^{d/2} + \text{volume terms} \end{aligned} \quad (63)$$

The volume terms contribute exchange terms in equations of motion, whereas the surface term in this equation implies that on both surfaces magnetization obeys the spin boundary condition:

$$\partial_x \mathbf{m} \Big|_{x=\pm d/2} = 0. \quad (64)$$

The variation of the Zeeman and dipolar Hamiltonians does not give the surface term since they do not contain derivatives of magnetization.

Returning to the amplitude representation, we identify as before the two components of magnetization with the Bogolyubov coefficients  $u$  and  $v$  at fixed  $\mathbf{q}$ . Thus, eq. (64) in amplitude representation is:

$$\partial_x u \Big|_{x=\pm d/2} = \partial_x v \Big|_{x=\pm d/2} = 0 \quad (65)$$

For the thick film and  $k_x \ell \ll 1$ , these equations imply that the magnitudes of coefficients at the evanescent waves  $A_m, B_m, C_m, D_m$  are less than the magnitudes of amplitudes of the bulk waves  $a, b, c, d$  by the factor  $\sim k_x \ell$ . [15] To see that, let us put all coefficients except of  $a, c$  and  $A_1, C_1$  equal to zero. Then equation (65) takes form:

$$(c - a) k_x \sin \frac{k_x d}{2} = (A_1 + C_1) \mathfrak{k}_1 \quad (66)$$

This equation proves the Sonin's statement since  $\mathfrak{k}_1 \sim 1/\ell$ . Nevertheless the evanescent waves allow to satisfy the MBC at fixed amplitudes of the bulk waves.

Neglecting in equations of motion (40) evanescent waves, we can rewrite them as:

$$\hat{\mathcal{M}} \begin{pmatrix} a \\ b \\ c \\ d \end{pmatrix} = 0, \quad (67)$$

where the  $4 \times 4$  matrix  $\hat{\mathcal{M}}$  is:

$$\hat{\mathcal{M}} = \begin{pmatrix} \omega - \mathcal{A} & 0 & \mathcal{B} & \mathcal{C} \\ 0 & \omega - \mathcal{A} & -\mathcal{C} & \mathcal{B} \\ -\mathcal{B} & \mathcal{C} & \omega + \mathcal{A} & 0 \\ -\mathcal{C} & -\mathcal{B} & 0 & \omega + \mathcal{A} \end{pmatrix}, \quad (68)$$

and

$$\begin{aligned} \mathcal{A} &= \gamma \left( \mathcal{H} + M\ell^2 k^2 + \frac{2\pi M(k_x^2 + k_y^2)}{k^2} \right) \\ \mathcal{B} &= \frac{2\pi\gamma M(k_x^2 - k_y^2)}{k^2} \\ \mathcal{C} &= \frac{4\pi\gamma M k_x k_y}{k^2} \end{aligned} \quad (69)$$

The determinant of the matrix  $\hat{\mathcal{M}}$  is

$$\det \hat{\mathcal{M}} = (\omega^2 - \mathcal{A}^2 + \mathcal{B}^2 + \mathcal{C}^2)^2. \quad (70)$$

It turns into zero at  $\omega = \sqrt{\mathcal{A}^2 - \mathcal{B}^2 - \mathcal{C}^2}$  that gives the obtained earlier dispersion relation (46). The eigenvalues  $\pm\omega$  of the matrix  $\hat{\mathcal{M}}$  are double degenerate. Therefore, their eigenvectors contain two independent coordinates, for example the amplitudes  $a$  and  $b$ , whereas two others are expressed as their linear combination as it follows from the equations (67):

$$\begin{aligned} c &= \frac{\mathcal{B}}{\omega \pm \mathcal{A}} a - \frac{\mathcal{C}}{\omega \pm \mathcal{A}} b \\ d &= \frac{\mathcal{C}}{\omega \pm \mathcal{A}} a + \frac{\mathcal{B}}{\omega \pm \mathcal{A}} b \end{aligned} \quad (71)$$

Note that the two eigenvectors corresponding to different signs in denominators are orthogonal at mass shell, i.e., at  $\omega = \sqrt{\mathcal{A}^2 - \mathcal{B}^2 - \mathcal{C}^2}$  and any choice of coordinates  $a$  and  $b$ .

Let us substitute the amplitudes  $c$  and  $d$  from eqs. (71) for the sign  $+$  into the first two of self-consistency equations (61). Then we find a system of two homogeneous equations of the form:

$$\begin{aligned} Pa + Qb &= 0 \\ Ra + Sb &= 0 \end{aligned} \quad (72)$$

where

$$\begin{aligned}
P &= \left[ q_y^2 - q^2 + \frac{(q_y^2 + q^2)\mathcal{B}}{\omega + \mathcal{A}} \right] f_1 - \frac{2q_y q \mathcal{C}}{\omega + \mathcal{A}} f_2 \\
Q &= \frac{(q_y^2 + q^2)\mathcal{C}}{\omega + \mathcal{A}} f_1 + \frac{2q_y q \mathcal{B}}{\omega + \mathcal{A}} f_2 \\
R &= -\frac{(q_y^2 + q^2)\mathcal{C}}{\omega + \mathcal{A}} f_1 + \frac{2q_y q \mathcal{C}}{\omega + \mathcal{A}} f_2 \\
S &= \left[ q_y^2 - q^2 + \frac{(q_y^2 + q^2)\mathcal{B}}{\omega + \mathcal{A}} \right] f_2 + \frac{2q_y q \mathcal{C}}{\omega + \mathcal{A}} f_1
\end{aligned} \tag{73}$$

The determinant of the system (72)  $PS - QR$  must be zero. It determines the quantization of  $k_x$ . Equation  $PS - QR = 0$  gives:

$$f_1^2 - f_2^2 = 2\Gamma f_1 f_2; \Gamma = \frac{(q_y^2 - q^2)\omega + (q_y^2 + q^2)\mathcal{B}}{2q_y q \mathcal{B}}. \tag{74}$$

From this equation we find:

$$\frac{f_1}{f_2} = \Lambda \equiv \Gamma \pm \sqrt{\Gamma^2 + 1}. \tag{75}$$

Note that the change of sign in front of square root turns  $\Lambda$  into  $-1/\Lambda$ . Employing equations (55,56), we represent the quantization condition in a more explicit form:

$$\tan \frac{k_x d}{2} = \frac{q - \Lambda k_x}{\Lambda q + k_x}. \tag{76}$$

The change  $\Lambda \rightarrow -1/\Lambda$  transforms the fraction  $\frac{q - \Lambda k_x}{\Lambda q + k_x}$  into inverse value with opposite sign, i.e.,  $-\frac{\Lambda q + k_x}{q - \Lambda k_x}$ . For the waves propagating along spontaneous magnetization ( $k_y = 0$ ), the quantization condition becomes

$$\tan \frac{k_x d}{2} = \frac{q}{k_x} \text{ or } \tan \frac{k_x d}{2} = -\frac{k_x}{q} \tag{77}$$

The first of them was first found by Damon and Eshbach [5] for purely dipolar interaction and reproduced by Sonin.[15] It corresponds to the pure cosine solution ( $b = 0$ ). The second sign at  $k_y = 0$  corresponds to the pure sine solution ( $a = 0$ ).[11] For general direction of propagation in-plane the two different signs in front of square root in eq. (75) correspond to two different branches of discrete solutions. We denote them by discrete index  $\nu$  accepting two values  $\pm$ .

### 3.5.2 Quantization of transverse wave vectors. Parallel propagation.

Equations (77) have a discrete set of solutions for  $k_{xn}$  in the intervals  $\left(\frac{\pi n}{d}, \frac{\pi(n+1/2)}{d}\right)$  for the cosine and in the intervals  $\left(\frac{\pi(n+1/2)}{d}, \frac{\pi(n+1)}{d}\right)$  for the sine transverse magnetization, where  $n$  is any non-negative integer. It is clearly seen from Fig. 2. In the limit  $qd \gg 1$  the approximate analytical solution is possible for  $n \ll qd$ .

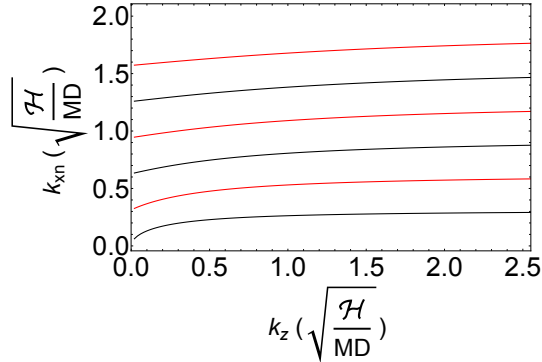


Figure 2: Plots of the dependence of quantized transverse wave vectors  $k_{xn}$  on  $k_z$  in units  $\sqrt{\frac{\mathcal{H}}{MD}}$  for  $d = 10$  in units  $\sqrt{\frac{MD}{\mathcal{H}}}$ . Black and red curves correspond to even and odd transverse modes, respectively

In this case  $k_x \ll q$  so the ratio  $\frac{q}{k_x} \gg 1$  for the first series of quantized  $k_x$ . Therefore,  $\frac{k_x d}{2}$  in the first equation (77) must be close to  $(n + \frac{1}{2})\pi$  and

$$k_{xn}^{(+)} \approx \frac{(2n+1)\pi}{d} \left(1 - \frac{2}{qd}\right) \quad (78)$$

Here we used the index + as notation of the first series (even transverse distribution of magnetization). For large  $n$  and  $qd \gg 1$  the approximate equation for the quantized values of the first series is:

$$k_{xn}^{(+)} \approx \frac{2n\pi}{d} + \frac{2}{d} \arctan \frac{qd}{2n\pi} \quad (79)$$

It accurately matches the result (78) for  $1 \ll n \ll qd$ .

For the second series the quantized transverse wave vectors for  $qd \gg 1$  and  $n \ll qd$  are

$$k_{xn}^{(-)} \approx \frac{2n\pi}{d} \left(1 - \frac{2}{qd}\right) \quad (80)$$

and for  $n \gg 1$

$$k_{xn}^{(-)} \approx \frac{(2n+1)\pi}{d} + \frac{2}{d} \arctan \frac{qd}{2n\pi} \quad (81)$$

### 3.5.3 Wave vectors and effective masses at minimum energy.

Two energy minima  $\pm Q$  are located on  $z$ -axis and correspond to minimal value  $n = 0$  and symmetric branch of the transverse momentum quantization, i.e.  $k_x \approx \frac{\pi}{d}$ . Let us minimize explicitly the energy or frequency eq. (46). For a thick film  $d \gg \ell$ , the energy is  $\varepsilon = \hbar\omega(\mathbf{q}, k_x)$ . It is more convenient to minimize



the square of energy

$$\varepsilon^2(\mathbf{q}, k_x) = \mu_B^2 \left( \mathcal{H}^2 + 2\mathcal{H}M\ell^2 k^2 + \frac{4\pi\mathcal{H}M(k_x^2 + k_y^2)}{k_z^2} \right). \quad (82)$$

We first minimize square of energy over  $q_y$  putting  $q_y = 0$  and in the square of total momentum  $k^2 = k_x^2 + q_y^2 + q_z^2$  neglect  $k_x^2$ . Taking derivative over  $q_z$  from  $\varepsilon^2(q_z, 0, k_x)$  at  $k_x = \frac{\pi}{d}$ , we get:

$$2\varepsilon \frac{\partial \varepsilon}{\partial q_z} = 4\mu_B^2 \mathcal{H}M \left( \ell^2 q_z - \frac{2\pi^3}{q_z^3 d^2} \right). \quad (83)$$

At minimum energy the derivative  $\frac{\partial \varepsilon}{\partial q_z} = 0$ . From this requirement we find, that two minima are located at  $q_z = \pm Q$ , where

$$Q = \frac{(2\pi^3)^{1/4}}{\sqrt{\ell d}}. \quad (84)$$

This result was obtained by E. Sonin.[15]

The main value of the mass tensor  $m_z$  in  $z$  direction relates to the second derivative  $\frac{\partial^2 \varepsilon}{\partial q_z^2}$  for  $q_z = \pm Q$  as  $m_z = \hbar^2 / \frac{\partial^2 \varepsilon}{\partial q_z^2} \Big|_{q_z=Q}$ . By differentiation of eq. (83) and putting  $q_z = Q$ ,  $\varepsilon_{\min} = \mu_B \mathcal{H}$ , we find:

$$m_z = \frac{\hbar^2}{8\mu_B M \ell^2} \quad (85)$$

To find  $m_y$ , we need to take the second derivative of  $\varepsilon^2(\mathbf{q}, k_x)$  given by eq. (82) over  $q_y$  at  $q_y = 0, q_z = Q$  neglecting  $k_x$ . The searched effective mass is  $m_y = \hbar^2 / \frac{\partial^2 \varepsilon}{\partial q_y^2} \Big|_{q_y=0}$ . An elementary calculation gives:

$$m_y = \frac{\hbar^2 Q^2}{8\pi\mu_B M} \quad (86)$$

The mass  $m_y$  is much less than  $m_z$ : their ratio is  $m_y/m_z = \ell/(\pi d) \ll 1$ . For the film of YIG 5 $\mu\text{m}$  thick  $Q \approx 6.44 \times 10^5 \text{ cm}^{-1}$ ,  $m_z = 7.37 \times 10^{-27} \text{ g}$ ;  $m_y = 1.78 \times 10^{-29} \text{ g}$ .

### 3.5.4 Quantization of transverse wave vector: arbitrary direction of propagation.

Despite of rather involved structure of quantization condition (76) its solution can be written explicitly in the limit  $d \gg \ell$ , and  $qd \gg 1$ . The roots of this equation are  $k_{x\nu n}$ , where  $n = 0, 1, 2, \dots$  is the number of quantized value  $k_x$ ,  $\nu = \pm$  stays for even or odd transverse distribution of magnetization. The explicit analytical expression for these roots in the asymptotic region and large  $n \gg 1$  is

$$k_{x\nu n} = \frac{2n\pi}{d} + \frac{2}{d} \arctan \frac{qd - 2\pi n \Lambda_{\nu n}}{qd \Lambda_{\nu n} + 2\pi n}. \quad (87)$$

To find parameters  $\Lambda_{\nu n} = \Gamma + \nu\sqrt{\Gamma^2 + 1}$  it is necessary to replace  $k_x$  by  $2\pi n/d$  in the equations (75) for  $\Lambda$  and (74) in all functions containing  $k_x$  in its arguments. Equation (87) has precision  $1/qd$  and is valid for  $1 \ll n \ll qd$ . In the entire this region the difference between the quantized values of  $k_x$  with the same number in the two branches is

$$k_{x+n} - k_{x-n} = \frac{\pi}{d} \quad (88)$$

The ratio of amplitudes in this range of variables is

$$\frac{b_{\nu n}}{a_{\nu n}} = -\frac{qA}{\omega}\Lambda_{\nu} - \frac{C}{\omega} \quad (89)$$

At fixed direction of in-plane propagation given by the angle  $\theta$  between the wave vector and direction of the spontaneous magnetization  $\mathbf{M}$ , the frequency as function of the wave vector magnitude has minimum at

$$q_0 = \frac{2\sqrt{\pi}\chi^{3/4}\sqrt{\cos\theta}}{(2 + \chi\sin^2\theta)^{1/4}}\sqrt{\frac{k_{x\nu n}}{\ell}}, \quad (90)$$

where  $\chi = \frac{4\pi M}{\mathcal{H}}$ . From this equation and strong inequality  $q\ell \ll 1$  it follows that  $q_0 \gg k_{x\nu n} \approx \frac{2\pi}{d}n$ .

### 3.5.5 Motion of energy minimum vs. $k_x$ .

At very large  $n \gg \frac{d}{\ell}$  the value  $k^2$  becomes so large that the exchange interactions dominates and the frequency of a magnon becomes equal to  $\omega = \gamma M\ell^2 k^2$ . Then the minimum energy occurs at  $q = 0$ . It means that the position of minimum of frequency  $q_0$  first grows with  $k_x$  and reaches its maximum at some specific  $k_{x1} \sim 1/\ell$ . At further growth of  $k_x$  the position of frequency minimum  $q_0(k_x)$  decreases and reaches zero at another specific value of  $k_x = k_{x2}$ . At further growth of  $n$  it remains zero. Theory gives exact analytical answers for all these values, namely:

$$k_{x1}^2 = \frac{1}{3}k_1^2 + \frac{2 + \chi}{12\pi}\tan^2\theta k_1^4\ell^2, \quad (91)$$

where

$$k_1^2 = \frac{\mathcal{H}}{6M\ell^2} \left[ \sqrt{(2 + \chi\sin^2\theta)^2 + 6\chi\cos\theta} - 2 - \chi\sin^2\theta \right]. \quad (92)$$

The maximal value of  $q_0$  is given by

$$q_{0\max}^2 = k_1^2 + k_{x1}^2. \quad (93)$$

Finally the value of  $k_x^2$  at which the minimum of frequency merges with maximum located at  $q = 0$  is

$$k_{x2}^2 = \frac{\mathcal{H}}{4M\ell^2} \left[ \sqrt{(2 + \chi\sin^2\theta)^2 + 8\chi\cos\theta} - 2 - \chi\sin^2\theta \right]. \quad (94)$$

The position of maximum  $k_0(k_x)$  for  $k_x \ell \gtrsim 1$  is given by

$$k_0^2(k_x) = \frac{\mathcal{H}}{M\ell^2} \frac{2 + \chi \sin^2 \theta}{2} w(\xi), \quad (95)$$

where  $w(\xi)$  is the solution of a cubic equation:

$$w^3 + w^2 = \xi \quad (96)$$

and

$$\xi = \frac{\chi^2 \cos^2 \theta k_x^2 \ell^2}{\pi (2 + \chi \sin^2 \theta)^3} \quad (97)$$

Details of these calculations can be found in the Appendix[motion of minima]. In the analysis of this subsection we followed the work [11].

### 3.6 Comparison with other calculations and experiment.

The results of numerical calculations of quantized spectra eq. (82) with quantized  $k_{xn}$  for propagation perpendicular and parallel to magnetization and  $d = 18.2$  in units  $\sqrt{\frac{MD}{\mathcal{H}}}$ ,  $\chi = 2.5$  are shown in Fig 3(a) and 3(b), spectra of the first transverse modes for a number of different directions of propagation specified by the angle  $\theta = \arctan \frac{k_y}{k_z}$  are shown in Fig. 3(c).

The spectra for parallel and perpendicular propagation (Fig. 3(a) and 3(b)) agree very well with the numerical calculations of the work [16] based on diagonalization of a large matrix. We also discovered an excellent agreement with similar calculations of the same work made for the YIG film with a thickness of  $5 \mu m$ .

Figure 4 shows a comparison of the theoretical spectrum with the experiment [17, 18]. Brillouin scattering spectroscopy was used in the experiment. Its precision is not sufficient for resolution of excited states. A dramatic increase in precision was achieved by an experimental group led by J. Ketterson [19]. His method makes use of direct microwave excitation of magnons via a specially designed antenna. It is made up of periodically repeated emitters that are powered by an adjustable frequency generator. The excited magnon wave-length coincides with the distance between emitters  $\lambda$ . The magnon frequency at this wave vector  $k_z = (2\pi)/\lambda$  is a frequency at which the resonance adsorption of microwave radiation reaches maximum. The increased resolution allowed for the observation of multiple magnon modes (up to nine). This is the first time that different transverse magnon modes have been experimentally observed. Figure 5 shows a comparison of theoretical spectrum with experimental results [19]. The agreement between theory and experiment is excellent.

### 3.7 Thin films.

In what follows till the end of this section we use  $\sqrt{M/\mathcal{H}}\ell$  as unit of length and  $(\gamma\mathcal{H})^{-1}$  as unit of time. In this part we discuss the case of thin films.

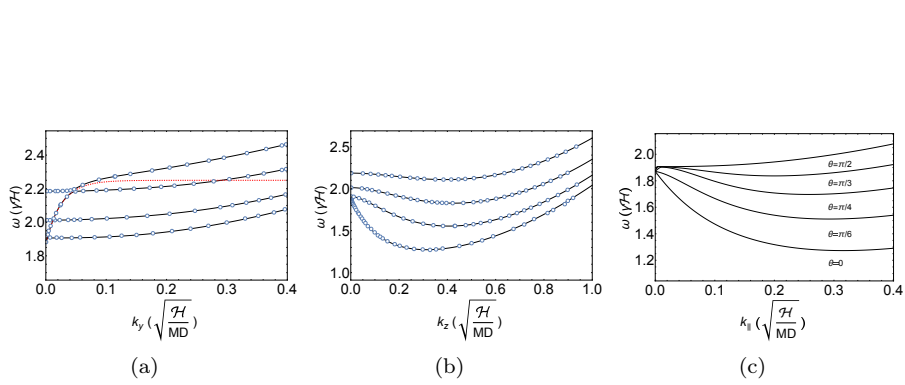


Figure 3: Results of numerical calculations for the case  $d = 18.2$  in units  $\sqrt{\frac{MD}{\mathcal{H}}}$  and  $\chi = 2.5$ . (a) The spectra of first four quantized modes for direction of propagation perpendicular to magnetization. (b) Spectra of the first four modes for direction of propagation parallel to magnetization. (c) Spectra of the first transverse modes for  $\theta = 0, \frac{\pi}{6}, \frac{\pi}{4}, \frac{\pi}{3}, \frac{\pi}{2}$ . Black solid curves correspond to our numerical calculations, red dashed line is the Damon-Eshbach surface mode, circles are numerical calculations by Kreisel *et al.* [16]. These figures agree with the figures from [11].

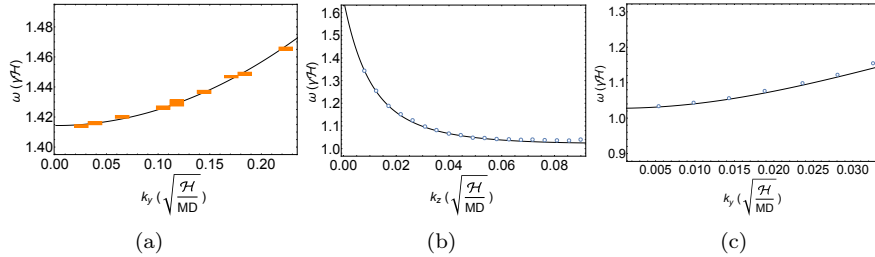


Figure 4: Comparison of theoretical spectrum with experiments. In experiments the Brillouin light scattering spectroscopy was used. (a) Comparison with A. A. Serga *et al.* [17]  $d = 5 \mu m$ ,  $H = 1750$  Oe. (b) Comparison with V. E. Demidov *et al.* [18]  $d = 5.1 \mu m$ ,  $H = 1000$  Oe for direction of propagation parallel to magnetization. (c) Comparison with V. E. Demidov *et al.* [18]  $d = 5.1 \mu m$ ,  $H = 1000$  Oe for fixed  $k_z = 3.4 \times 10^4 cm^{-1}$ . These figures agree with the figures from [11].

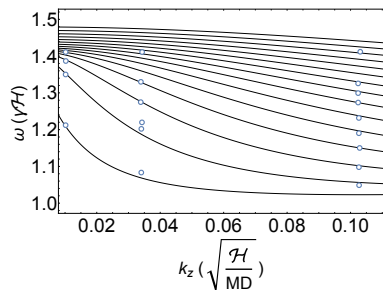


Figure 5: Comparison of theoretical spectrum with experiment. Solid curves are our calculations of the first 15 transverse modes for the YIG film of thickness  $5\mu\text{m}$ ,  $4\pi M = 1940$  Oe and  $H = 1960$  Oe. Circles on them are frequencies measured by J. Lim *et al.* [19] at three fixed wavelengths for different transverse mode. This figure agrees with the figure from [11].

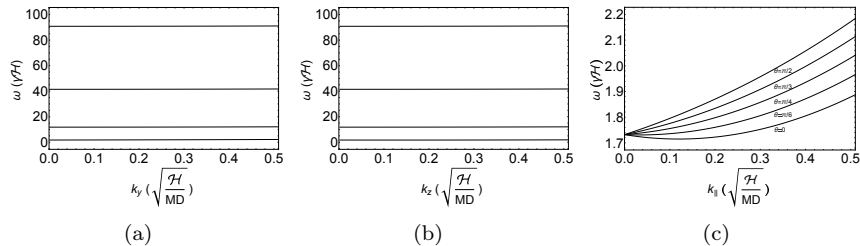


Figure 6: Results of numerical calculations for a thin film  $d = 1$  in units  $\sqrt{\frac{MD}{H}}$  and  $\chi = 2$ . (a) The spectra of first four quantized modes for direction of propagation perpendicular to magnetization. (b) Spectra of the first four modes for direction of propagation parallel to magnetization. (c) Spectra of the first transverse modes for  $\theta = 0, \frac{\pi}{6}, \frac{\pi}{4}, \frac{\pi}{3}, \frac{\pi}{2}$ . These figures agree with the figures from [11].

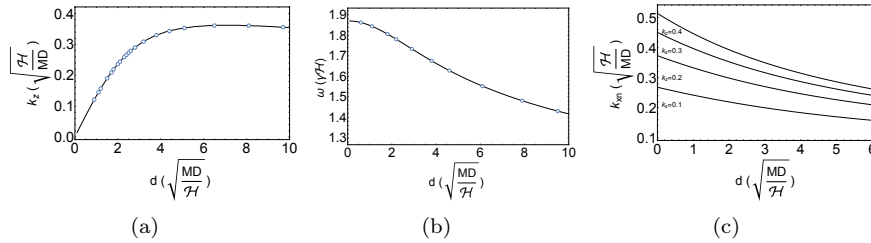


Figure 7: Results of numerical calculations for the case  $\chi = 2.5$  and  $\theta = 0$ . (a) Position of minima for the lowest mode vs  $d$  for thin films. (b) The value of frequency in minimum for the lowest mode vs  $d$  for thin films. (c)  $k_{xn}$  for the lowest mode vs  $d$  at fixed  $k_z = 0.1, 0.2, 0.3, 0.4$ . Black solid curves correspond to our numerical calculations, circles are numerical calculations by Kreisel *et al.* [16]. These figures agree with the figures from [11].

If the film's thickness is of the order of one or less ( $\ell$  in dimensional units), it is regarded as thin. The experimental realization of ultrathin films of YIG with  $d \ll 1$  looks very improbable since the typical value of  $\ell$  (in YIG) is a few tens of nanometers. It may be accomplished in thin, monolayer-thick ferromagnetic materials. Transverse modes with high  $n$  in thin films with  $d \sim 1$  have  $k_{xn} \approx \pi n/d \gg 1$  in the exchange dominance area. Thus, only a few modes with the lowest frequencies are of theoretical and experimental relevance. In these modes, evanescent waves penetrate to the film at a depth of the same order of magnitude as its thickness. They therefore play an equally essential role in spectral characteristics and TDM as the oscillating wave.

A compact analytic expression has been found only for frequency as function of the wave vector (see eq. (46)).

Fig. 6 shows examples of spectra in thin films that are qualitatively similar to spectra in thick films. Each mode determined by numbers  $\nu, n$  at not very big  $n$  has a frequency minimum at some  $k_{\parallel} \neq 0$ , but it does not follow equation  $\frac{\partial \omega^2}{\partial k_{\parallel}^2} = 0$  since  $k_{xn}$  also depends on  $k_{\parallel}$ . Fig. 6(a) and Fig. 6(b) show that at  $d = 1$ , the energy of transverse excitation weakly depends on  $k_z$ , a feature that could be expected for ultrathin films.

The graphs of position of minima and the value of frequency in minimum for the lowest mode vs  $d$  for thin films are shown in Fig.7. In the same figures 7(a) and 7(b), we compared our results with calculations of the same values by Kreisel *et al.* [16]. Finally, the graphs of  $k_{xn}$  for the lowest mode vs  $d$  at fixed  $k_{\parallel}$  and  $\theta = 0$  are shown in Fig. 7(c). An example of TDM for lowest mode and first excited mode in thin films is shown in Fig. 8.

All ground state spectra cross at the point  $k_{\parallel} = 0, \omega \approx \sqrt{1 + \chi}$  ( $\sqrt{3} \approx 1.73$  for  $\chi = 2$ ), exactly the same result as for the thick film. This is manifestation of a general property of films with arbitrary thickness: at  $\mathbf{k}_{\parallel} = 0$ , the transverse wave vector of the lowest transverse mode is also equal to zero. The frequency of the lowest mode equals to  $\omega_0 = \sqrt{1 + \chi}$  (ferromagnetic resonance frequency).

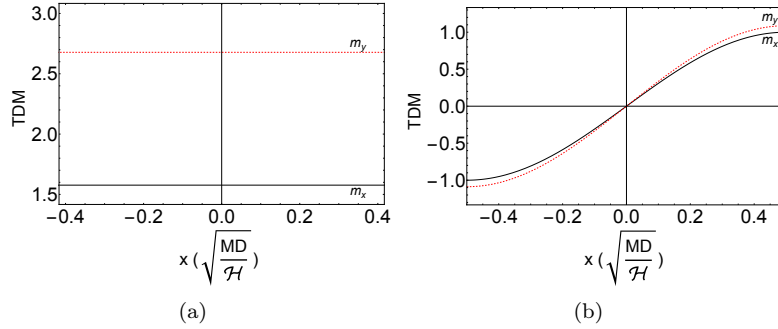


Figure 8: For the case  $\chi = 2$  and  $\theta = 0$  (a) TDM for the lowest mode at  $k_{\parallel} = 0.1$  and  $a_{1x} = 1$ . (b) TDM for the first excited mode at  $k_{\parallel} = 0.1$  and  $b_{1x} = 1$ . These figures agree with the figures from [11].

We consider first the limiting case of ultrathin films  $d \rightarrow 0$  when  $\theta = 0$ . It will be shown that only wave vectors of the lowest transverse mode with  $\nu = -, n = 0$  remains finite in this limit. All excited transverse state with other  $\nu$  or  $n$  have wave vectors that go to infinity as  $1/d$ . We just take into account the simplest scenario of waves propagating along magnetization and magnetic field in order to simplify calculations. The transverse mode then has a definite parity.

In such a case, the non-zero amplitudes are  $\mathbf{a}_i$  for even modes and  $\mathbf{b}_i$  for odd modes. For finite wave vectors  $\mathbf{k}_i$  in the taken limit,  $\sin k_{ix}d/2 \approx k_{ix}d/2$  and  $\cos k_{ix}d/2 \approx 1$  are appropriate values. This fact simplifies the SBC (64) and self-consistency equations (61). The second simplification results from the fact that the relationship between the  $x$  and  $y$  components of the vectors  $\mathbf{a}_i$  and  $\mathbf{b}_i$  is reduced to  $a_{iy} = \frac{\omega}{1+k_i^2} a_{ix}$  and  $b_{iy} = \frac{\omega}{1+k_i^2} b_{ix}$ , respectively. Here we denote three kernels of cubic equation for  $k^2$  (45) as  $k_1^2, k_2^2, k_3^2$  and corresponding vector amplitudes at  $\sin(k_{ix}x)$  and  $\cos(k_{ix}x)$  as  $\mathbf{a}_i, \mathbf{b}_i$ . Let us remind that  $k_1^2 > 0$ , whereas  $k_2^2, k_3^2 < 0$ . After all these simplifications, the quantization of an even mode is described by the system of three equations with three independent amplitudes  $a_{ix}$  :

$$\begin{cases} \sum_{i=1}^3 k_{ix}^2 a_{ix} = 0 \\ \sum_{i=1}^3 \frac{k_{ix}^2}{1+k_i^2} a_{ix} = 0 \\ \sum_{i=1}^3 \frac{a_{ix}}{k_i^2} = 0 \end{cases} \quad (98)$$

Zeros of determinant of this system determine quantized values of  $k_{xn}^2$ . In order to transform this determinant into an explicit function of  $k_{xn}$  one should employ the relations  $k_1^2 = k_{xn}^2 + k_z^2$ ,

$$k_{2,3}^2 = -1 - \frac{\chi}{2} - \frac{k_1^2}{2} \pm \sqrt{\left(1 + \frac{\chi}{2} + \frac{k_1^2}{2}\right)^2 - \frac{\chi k_z^2}{k_1^2}} \quad (99)$$

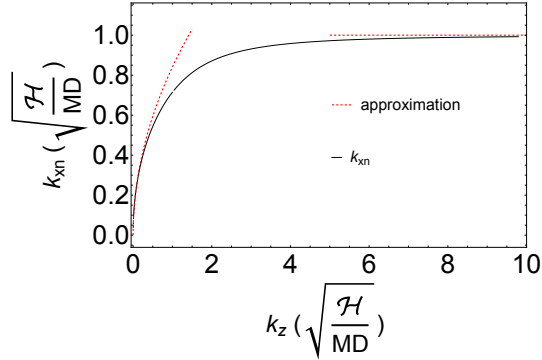


Figure 9: Plot of  $k_{xn}$  at  $d \rightarrow 0$  and approximation to it when  $\chi = 2$  and  $\theta = 0$ . This figure agrees with the figure from [11].

and  $k_{ix}^2 = k_i^2 - k_z^2$ . The only positive root of this equation at small  $k_z \ll 1$  is

$$k_{xn} \approx \left( \frac{\chi}{2 + \chi} \right)^{1/4} \sqrt{k_z} \quad (100)$$

At large  $k_z$ ,  $k_{xn}$  asymptotically approaches a constant value  $k_{xn} \approx \sqrt{\chi/2}$ . Both these asymptotic values agree very well with numerical calculations of the dependence of  $k_{xn}$  on  $k_z$  at  $d \rightarrow 0$  (see Fig.9). The fact that  $k_{xn} = 0$  at  $k_z = 0$  is confirmed by the asymptotic behavior of  $k_{xn}$  at small  $k_z$ . As a result, both in the limit of small  $d$  and the limit of large  $d$ , the value of frequency at  $k_{\parallel} = 0$  is  $\sqrt{1 + \chi}$ . On Fig. 10, the plots of  $k_{xn}$  vs.  $k_z$  at  $d = 1$  and  $d = 0$  are compared.

We can now demonstrate the general proposition that, regardless of thickness, the frequency of the lowest mode at  $\mathbf{k}_{\parallel} = 0$  equals  $\sqrt{1 + \chi}$ . Set  $k_y = 0$  and consider  $k_z \ll 1/d^2$ . We will show that the same equation (100) determines the first quantized value  $k_{xn}$ , but the arguments must be modified. In order to prove the result (100), let us assume that the initial quantized value of  $k_{xn}$  obeys the strong inequalities  $k_z \ll k_{xn} \ll 1$ . Then eq. (99) implies that  $k_{2x}^2 \approx -\chi k_z^2 / [(2 + \chi) k_{xn}^2]$  has small magnitude, whereas  $k_{3x}^2 \approx -2 - \chi$  has the magnitude of the order of unity. Let us first consider the SBC (64) that in considered situation take form

$$\begin{aligned} k_{xn}^2 a_{1x} + k_{2x}^2 a_{2x} - \sqrt{2 + \chi} \frac{2 \sinh \sqrt{2 + \chi} d / 2}{d} a_{3x} &= 0 \\ k_{xn}^2 a_{1x} + k_{2x}^2 a_{2x} + \frac{2 \sqrt{2 + \chi} \sinh \sqrt{2 + \chi} d / 2}{(1 + \chi) d} a_{3x} &= 0 \end{aligned} \quad (101)$$

These equations imply  $a_{3x} = 0$ . Then they become identical and define the ratio  $a_{2x}/a_{1x} = -k_{xn}^2/k_{2x}^2$ . Next consider the self-consistency equations that in the same limit have a form:

$$\frac{a_{1x}}{k_1^2} + \frac{a_{2x}}{k_2^2} = 0$$



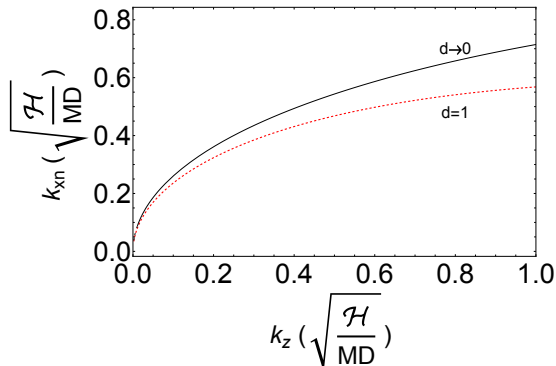


Figure 10:  $k_{xn}$  vs.  $k_z$  for the lowest mode at  $d \rightarrow 0$  and  $d = 1$  at  $\chi = 2$  and  $\theta = 0$ . This figure agrees with the figure from [11].

Using the previously found ratio  $a_{1x}/a_{2x}$ , we again obtain eq. (100) for this more general situation. It shows that in the limit  $k_z \rightarrow 0$ , the limit of ratio  $k_z^2/k_{xn}^2$  is also zero and limiting value of  $\omega$  is  $\sqrt{1+\chi}$  independently on thickness. Note that in the limit  $\mathbf{k}_{\parallel} = 0$  the magnetization in the lowest spin-wave mode does not depend on transverse coordinate.

Although thin films are more sensitive to the exact form of the SBC than thick films, changing forms of these requirements have no effect on the symmetry or general features of solutions. An important problem is how the wave vector  $k_{z\min}$  corresponding to the minimum of energy changes with thickness. For thick films it behaves as  $1/\sqrt{d}$  [15] and grows when film becomes thinner. However, in the case of ultrathin films, it decreases linearly with thickness.

It means that the wave vector  $k_{z\min}$  as function of  $d$  has a maximum. According to numerical calculations shown in Fig. 7(a) for  $\chi = 2.5$  the maximum is located at  $d \approx 6$ , and the maximum value of  $k_{z\min}$  is around 0.3. For  $d = 5\mu\text{m}$  and  $\chi = 2$ ,  $k_{z\min}$  is around 0.02. Thus, by decreasing thickness from  $5\mu\text{m}$  to 15–30 nm, the wave vector  $k_{z\min}$  may be modified by a factor of roughly 15. The size of any soliton-like formation constructed of magnons that may be utilized for information transfer without dissipation or with very little dissipation has an upper limit determined by the minimal wavelength of a magnon, according to [20].

## 4 Interaction of magnons.

Previously we considered only quadratic in amplitudes part of the Hamiltonian. Here we take into account higher order contributions, i.e, we consider the magnon interaction. The expansion will be limited by the terms of the third and the fourth order. The expansion must be applied only to the exchange (17) and dipolar (19) Hamiltonians since the Zeeman Hamiltonian is purely quadratic.

### 4.1 Third order terms.

Let us first write out the 3rd order terms of the Hamiltonian, which come solely from the dipolar part:

$$H_{d3} = -\frac{\mu_B \sqrt{2\mu_B M}}{2} \iint \left( |\psi|^2 + \frac{1}{4} |\psi'|^2 \right) \partial_z (\psi' \partial'_- + \psi'^* \partial'_+) \frac{dV dV'}{|\mathbf{r} - \mathbf{r}'|}. \quad (102)$$

In terms of the Fourier transforms defined by eq. (23) and employing the identity

$$\frac{1}{|\mathbf{r} - \mathbf{r}'|} = \frac{4\pi}{A} \sum_{\mathbf{q}} e^{i\mathbf{q}(\mathbf{r}-\mathbf{r}')} G_q(x-x'), \quad (103)$$

where the 1d Green function is defined by eq. (29), we find:

$$\begin{aligned} H_{d3} = & -\frac{2\pi\mu_B\sqrt{2\mu_B M}}{\sqrt{A}} \iint_{-\infty}^{\infty} dx dx' \\ & \sum_{\mathbf{q}_1, \mathbf{q}_2, \mathbf{q}_3, \mathbf{q}} \left( \chi_{\mathbf{q}_1} \chi_{\mathbf{q}_2}^* \delta_{\mathbf{q}_1 - \mathbf{q}_2 + \mathbf{q}} \delta_{\mathbf{q}_3 - \mathbf{q}} \right. \\ & \left. + \frac{1}{4} \chi'_{\mathbf{q}_1} \chi'_{\mathbf{q}_2} \delta_{\mathbf{q}} \delta_{\mathbf{q}_1 - \mathbf{q}_2 + \mathbf{q}_3 - \mathbf{q}} \right) i q_z \times \\ & [\chi'_{\mathbf{q}_3} (d_{x'} - q_y) + \chi'^*_{-\mathbf{q}_3} (d_{x'} + q_y)] G_q(x-x') \end{aligned} \quad (104)$$

The second term in the sum contains the factor  $\delta_{\mathbf{q}}$  that makes  $q_y = q_z = 0$ . Thus, the square bracket in this equation is equal to  $(\chi'_{\mathbf{q}_3} + \chi'^*_{-\mathbf{q}_3}) d_{x'}$ . Acting to  $G_q(x-x')$ , the operator  $d_{x'}$  transforms it into  $q \text{sign}(x-x') G_q(x-x') = \frac{\text{sign}(x-x')}{2}$ . Thus, the second term in the sum is zero. The Kronecker  $\delta$ -symbols in the first term imply that  $\mathbf{q} = \mathbf{q}_3 = \mathbf{q}_2 - \mathbf{q}_1$ . Thus, the dipolar Hamiltonian of the third order is simplified to

$$\begin{aligned} H_{d3} = & -\frac{2\pi\mu_B\sqrt{2\mu_B M}}{\sqrt{A}} \iint_{-\infty}^{\infty} dx dx' \\ & \sum_{\mathbf{q}_1, \mathbf{q}_2} \chi_{\mathbf{q}_1} \chi_{\mathbf{q}_2}^* i (q_{2z} - q_{1z}) [\chi'_{\mathbf{q}_2 - \mathbf{q}_1} (d_{x'} - q_{2y} + q_{1y}) \\ & + \chi'^*_{\mathbf{q}_1 - \mathbf{q}_2} (d_{x'} + q_{2y} - q_{1y})] G_{|\mathbf{q}_1 - \mathbf{q}_2|}(x-x') \end{aligned} \quad (105)$$

#### 4.1.1 Third order non-linearity in terms of quantized magnon amplitudes.

In this section we perform the Bogoliubov transformation (37) from transverse modes  $\chi_{\mathbf{q}}(x)$  to the quantized amplitudes of magnons  $\eta_{\mathbf{q},n}, \eta_{\mathbf{q},n}^*$ . After some algebra we arrive at a cubic form for these amplitudes limited by the requirement of the momentum conservation (translational invariance):

$$\begin{aligned} H_{d3} = & -\frac{2\pi\mu_B\sqrt{2\mu_B M}}{\sqrt{A}} \sum_{\mathbf{q}_1 n_1; \mathbf{q}_2 n_2; \mathbf{q}_3 n_3} \delta_{\mathbf{q}_1 - \mathbf{q}_2 + \mathbf{q}_3} \\ & \left( I_{d3}^{(++++)} \eta_{\mathbf{q}_1 n_1} \eta_{-\mathbf{q}_2 n_2} \eta_{\mathbf{q}_3 n_3} + I_{d3}^{(++-)} \eta_{\mathbf{q}_1 n_1} \eta_{-\mathbf{q}_2 n_2} \eta_{-\mathbf{q}_3 n_3}^* \right. \\ & \left. I_{d3}^{(+-+)} \eta_{\mathbf{q}_1 n_1} \eta_{\mathbf{q}_2 n_2}^* \eta_{\mathbf{q}_3 n_3} + I_{d3}^{(-++)} \eta_{-\mathbf{q}_1 n_1}^* \eta_{-\mathbf{q}_2 n_2} \eta_{\mathbf{q}_3 n_3} + c.c \right), \end{aligned} \quad (106)$$

where the eight coefficients  $I_{d3}^{(\rho\sigma\tau)}$  with  $\rho, \sigma, \tau$  taking values  $+, -$  are matrix elements of the three transverse modes: the first is  $u_{\mathbf{q}_1 n_1}^*(x)$  for  $\rho = +$  and

$u_{-\mathbf{q}_1 n_1}$  for  $\rho = -$ ; the second is  $v_{-\mathbf{q}_2 n_2}^*(x)$  for  $\sigma = +$  and  $v_{\mathbf{q}_2 n_2}$  for  $\sigma = -$ ; the third is given by

$$iq_{3z} [u_{\mathbf{q}_3 n_3}^*(x') (d_{x'} - q_{3y}) - v_{\mathbf{q}_3 n_3}^*(x') (d_{x'} + q_{3y})] G_{q_3}(x - x')$$

for  $\tau = +$  and

$$iq_{3z} [u_{-\mathbf{q}_3 n_3}(x') (d_{x'} + q_{3y}) - v_{-\mathbf{q}_3 n_3}(x') (d_{x'} - q_{3y})] G_{q_3}(x - x')$$

for  $\tau = -$ .

The matrix element is the double integral over  $x$  and  $x'$  from the products of any set of these three modes.

For the reader convenience we place below explicit expressions for the integrals  $I_{d3}^{(\rho\sigma\tau)}$  with all three indices + and with two + and one -:

$$\begin{aligned} I_{d3}^{(+++)} &= -iq_{3z} \iint dx dx' u_{\mathbf{q}_1 n_1}^* v_{-\mathbf{q}_2 n_2}^* \times \\ & [u_{\mathbf{q}_3 n_3}'^*(d_{x'} - q_{3y}) - v_{\mathbf{q}_3 n_3}'^*(d_{x'} + q_{3y})] G_{q_3}(x - x') \\ I_{d3}^{(++-)} &= -iq_{3z} \iint dx dx' u_{\mathbf{q}_1 n_1}^* v_{-\mathbf{q}_2 n_2}^* \times \\ & [u_{-\mathbf{q}_3 n_3}'(d_{x'} + q_{3y}) - v_{-\mathbf{q}_3 n_3}'(d_{x'} - q_{3y})] G_{q_3}(x - x') \\ I_{d3}^{(+--)} &= iq_{3z} \iint dx dx' u_{\mathbf{q}_1 n_1}^* v_{\mathbf{q}_2 n_2} \times \\ & [u_{\mathbf{q}_3 n_3}'^*(d_{x'} - q_{3y}) - v_{\mathbf{q}_3 n_3}'^*(d_{x'} + q_{3y})] G_{q_3}(x - x') \\ I_{d3}^{(-++)} &= iq_{3z} \iint dx dx' u_{-\mathbf{q}_1 n_1} v_{-\mathbf{q}_2 n_2}^* \times \\ & [u_{\mathbf{q}_3 n_3}'(d_{x'} - q_{3y}) - v_{\mathbf{q}_3 n_3}'(d_{x'} + q_{3y})] G_{q_3}(x - x') \end{aligned} \quad (107)$$

In order to obtain the Hamiltonian  $H_{d3}$  (106) and coefficients  $I_{d3}^{(\sigma\rho\tau)}$  we have used the fact that some terms (e.g. the term with  $\eta_{-\mathbf{q}_1 n_1}^* \eta_{\mathbf{q}_2 n_2}^* \eta_{-\mathbf{q}_3 n_3}^*$ ) can be expressed as complex conjugates of others (e.g. the term with  $\eta_{\mathbf{q}_1 n_1} \eta_{-\mathbf{q}_2 n_2} \eta_{\mathbf{q}_3 n_3}$ ) by permutation of the summation indices  $\mathbf{q}_1 \leftrightarrow \mathbf{q}_2$  that implies  $\mathbf{q}_3 \rightarrow -\mathbf{q}_3$ . Later we will use this kind of relations when calculating 4th-order terms. Note also that the three terms involving one complex conjugated function in eq. (106) can also be received each from other by renaming the summation indices. Thus, these three sums are identical. On the other hand two last of them are complex conjugates each to other. Therefore, all these sums are real.

#### 4.1.2 Cherenkov radiation of a low energy magnon by the high energy magnons.

In the theory of BECM the life-time of the condensate magnons is dominantly determined by their merging with a high energy magnon and by the inverse process of the Cherenkov radiation of the condensate magnon by a high energy magnons. Here we consider a more general problem when the high energy magnon emits or absorbs a low energy magnon. The high-energy magnon is assumed to have the exchange dominated dispersion  $\omega_{\mathbf{q}, k_x} = \gamma \ell^2 k^2$ , whereas the low-energy magnon dispersion is given by eq. (46). In the Bogoliubov coefficients  $u_{\mathbf{q}n}$  the coefficients  $a, b$  dominate for  $\nu = +$ ,  $c, d$  dominate for  $\nu = -$ , whereas  $v_{\mathbf{q}n} = 0$ . For low-energy magnons generally the coefficients  $a, b, c, d$

are of the same order of magnitude. They are defined by eqs. (49,50). For thick films in the integrals (107) defining the matrix elements of the Cherenkov or inverse Cherenkov process, the terms corresponding to evanescent waves can be neglected.

## 4.2 Fourth order terms.

Here we consider the 4th order terms of the Hamiltonian. In terms of general magnon wave function  $\psi(\mathbf{r})$  they are:

$$\begin{aligned}
H_4 &= H_{ex4} + H_{d4} \\
H_{ex4} &= \frac{\mu_B^2 \ell^2}{2} \int \left[ -|\psi|^2 |\nabla \psi|^2 + \frac{1}{2} \left( \nabla (|\psi|^2) \right)^2 \right] dV, \\
H_{d4} &= \frac{\mu_B^2}{2} \iint \left[ |\psi|^2 |\psi'|^2 \partial_z \partial'_z - \frac{1}{4} |\psi|^2 (\psi \partial_- + \psi^* \partial_+) (\psi' \partial'_- + \psi'^* \partial'_+) \right] \frac{dV dV'}{|\mathbf{r} - \mathbf{r}'|} \quad (108)
\end{aligned}$$

### 4.2.1 Fourth order Hamiltonian in terms of magnon amplitudes $\chi_{\mathbf{q}}(\mathbf{r})$ .

Employing Fourier transformation to the wave vector representation (23), we find the following expressions for  $H_{ex4}$  and  $H_{d4}$ :

$$\begin{aligned}
H_{ex4} &= \frac{\mu_B^2 \ell^2}{2A^2} \int \sum_{\mathbf{q}_1, \mathbf{q}_2, \mathbf{q}_3, \mathbf{q}_4} \left[ -\chi_{\mathbf{q}_1} \chi_{\mathbf{q}_2}^* (d_x \chi_{\mathbf{q}_3} d_x \chi_{\mathbf{q}_4}^* + \mathbf{q}_3 \mathbf{q}_4 \chi_{\mathbf{q}_3} \chi_{\mathbf{q}_4}^*) \right. \\
&\quad \left. + \frac{1}{2} d_x (\chi_{\mathbf{q}_1} \chi_{\mathbf{q}_2}^*) d_x (\chi_{\mathbf{q}_3} \chi_{\mathbf{q}_4}^*) + \frac{1}{2} (\mathbf{q}_1 - \mathbf{q}_2) (\mathbf{q}_3 - \mathbf{q}_4) \chi_{\mathbf{q}_1} \chi_{\mathbf{q}_2}^* \chi_{\mathbf{q}_3} \chi_{\mathbf{q}_4}^* \right] e^{i(\mathbf{q}_1 - \mathbf{q}_2 + \mathbf{q}_3 - \mathbf{q}_4) \mathbf{r}} dV \\
&= \frac{\mu_B^2 \ell^2}{4A} \int \sum_{\mathbf{q}_1, \mathbf{q}_2, \mathbf{q}_3, \mathbf{q}_4} \left[ d_x \chi_{\mathbf{q}_1} \chi_{\mathbf{q}_2}^* d_x \chi_{\mathbf{q}_3} \chi_{\mathbf{q}_4}^* + \chi_{\mathbf{q}_1} d_x \chi_{\mathbf{q}_2}^* \chi_{\mathbf{q}_3} d_x \chi_{\mathbf{q}_4}^* \right. \\
&\quad \left. - (\mathbf{q}_1^2 + \mathbf{q}_2^2) \chi_{\mathbf{q}_1} \chi_{\mathbf{q}_2}^* \chi_{\mathbf{q}_3} \chi_{\mathbf{q}_4}^* \right] \delta_{\mathbf{q}_1 - \mathbf{q}_2 + \mathbf{q}_3 - \mathbf{q}_4} d\mathbf{x} \\
&= \frac{\mu_B^2 \ell^2}{4A} \int \sum_{\mathbf{q}_1, \mathbf{q}_2, \mathbf{q}_3, \mathbf{q}_4} \left[ d_x \chi_{\mathbf{q}_1} \chi_{\mathbf{q}_2}^* d_x \chi_{\mathbf{q}_3} \chi_{\mathbf{q}_4}^* + \chi_{\mathbf{q}_1} d_x \chi_{\mathbf{q}_2}^* \chi_{\mathbf{q}_3} d_x \chi_{\mathbf{q}_4}^* \right. \\
&\quad \left. - \frac{1}{2} (\mathbf{q}_1^2 + \mathbf{q}_2^2 + \mathbf{q}_3^2 + \mathbf{q}_4^2) \chi_{\mathbf{q}_1} \chi_{\mathbf{q}_2}^* \chi_{\mathbf{q}_3} \chi_{\mathbf{q}_4}^* \right] \delta_{\mathbf{q}_1 - \mathbf{q}_2 + \mathbf{q}_3 - \mathbf{q}_4} d\mathbf{x} \quad (109)
\end{aligned}$$

$$\begin{aligned}
H_{d4} &= \frac{2\pi \mu_B^2}{A^3} \iint \sum_{\mathbf{q}_1, \mathbf{q}_2, \mathbf{q}_3, \mathbf{q}_4, \mathbf{q}} \left\{ q_z^2 \chi_{\mathbf{q}_1} \chi_{\mathbf{q}_2}^* \chi'_{\mathbf{q}_3} \chi'^*_{\mathbf{q}_4} e^{i[(\mathbf{q}_1 - \mathbf{q}_2) \mathbf{r} + (\mathbf{q}_3 - \mathbf{q}_4) \mathbf{r}' + \mathbf{q}(\mathbf{r} - \mathbf{r}')] } - \right. \\
&\quad \left. \frac{1}{4} \chi_{\mathbf{q}_1} \chi_{\mathbf{q}_2}^* [\chi_{\mathbf{q}_3} (d_x + q_y) + \chi_{-\mathbf{q}_3}^* (d_x - q_y)] [\chi'_{\mathbf{q}_4} (d_{x'} - q_y) + \chi'^*_{-\mathbf{q}_4} (d_{x'} + q_y)] \right. \\
&\quad \left. \times e^{i[(\mathbf{q}_1 - \mathbf{q}_2) \mathbf{r} + \mathbf{q}_3 \mathbf{r} + \mathbf{q}_4 \mathbf{r}' + \mathbf{q}(\mathbf{r} - \mathbf{r}')] } \right\} G_q(x - x') dV dV' \quad (110)
\end{aligned}$$

After integration over  $y, z$  and  $y', z'$  the 4th-order dipolar Hamiltonian transforms into the sum over momenta and integral over transverse coordinates:

$$\begin{aligned}
H_{d4} &= \frac{2\pi \mu_B^2}{A} \iint \sum_{\mathbf{q}_1, \mathbf{q}_2, \mathbf{q}_3, \mathbf{q}_4, \mathbf{q}} \left\{ q_z^2 \chi_{\mathbf{q}_1} \chi_{\mathbf{q}_2}^* \chi'_{\mathbf{q}_3} \chi'^*_{\mathbf{q}_4} \delta_{\mathbf{q}_1 - \mathbf{q}_2 + \mathbf{q}} \delta_{\mathbf{q}_3 - \mathbf{q}_4 - \mathbf{q}} \right. \\
&\quad \left. - \frac{1}{4} \chi_{\mathbf{q}_1} \chi_{\mathbf{q}_2}^* [\chi_{\mathbf{q}_3} (d_x + q_y) + \chi_{-\mathbf{q}_3}^* (d_x - q_y)] [\chi'_{\mathbf{q}_4} (d_{x'} - q_y) + \chi'^*_{-\mathbf{q}_4} (d_{x'} + q_y)] \right. \\
&\quad \left. \times \delta_{\mathbf{q}_1 - \mathbf{q}_2 + \mathbf{q}_3 + \mathbf{q}} \delta_{\mathbf{q}_4 - \mathbf{q}} \right\} G_q(x - x') dx dx'. \quad (111)
\end{aligned}$$

In these calculation we used the symmetry with respect to permutations of running momenta participating in the sum and the relation between Fourier component of  $1/|\mathbf{r} - \mathbf{r}'|$  and one-dimensional Green function  $G_q(x - x')$  (see eq. (29)).

#### 4.2.2 Fourth order Hamiltonian in terms of the magnon amplitudes

$$\eta_{\mathbf{q}\nu n}.$$

Employing the Bogoliubov transformation (38), we represent the 4-th order Hamiltonian in terms of the homogeneous fourth order polynomials of the form (the subscripts  $\mathbf{q}_i, n_i$  in the coefficients  $I_4$  are omitted for brevity):

$$H_4 = \sum_{\mathbf{q}_i n_k \rho_l (i,k,l=1\dots 4)} I_4^{(\rho_1 \rho_2 \rho_3 \rho_4)} \left[ \prod_{j=1}^4 \eta_{\mathbf{q}_j n_j}^{(\rho_j)} \right] \delta_{\mathbf{q}_1 + \mathbf{q}_2 + \mathbf{q}_3 + \mathbf{q}_4}, \quad (112)$$

where  $\eta_{\mathbf{q}n}^{(+)} = \eta_{\mathbf{q}n}; \eta_{\mathbf{q}n}^{(-)} = \eta_{\mathbf{q}n}^*$ . It is obvious that the matrix  $I_4$  can be made invariant under permutation of four its composite indices  $\gamma_j = (\rho_j \mathbf{q}_j n_j); j = 1, 2, 3, 4$  since the product in eq. (112) is invariant under such permutation. Therefore, it is more reasonable to denote the matrix elements of the matrix  $I_4$  as  $(I_4)_{\gamma_1 \gamma_2 \gamma_3 \gamma_4}$ . The table of coefficients  $(I_4)_{\gamma_1 \gamma_2 \gamma_3 \gamma_4}$  is given in the Appendix [Hamiltonian of the 4-th order].

#### 4.2.3 Interaction of condensate magnons in thick films.

Here we show the results of calculations of the interaction between condensate of magnons that have momenta either  $\mathbf{Q} = Q\hat{z}$  or  $-\mathbf{Q}$ . When the condensate exists, the chemical potential  $\mu$  is equal to the minimal magnon energy  $\Delta$ . Therefore the wave functions of the condensates  $\psi_{\pm\mathbf{Q}}$  do not depend on time (we remind that the time dependence of the wave function is given by  $\exp\left[-\frac{i(\Delta-\mu)t}{\hbar}\right]$ ). Further for brevity we denote the wave functions of the two condensates as  $\psi_{\pm}$  and present them in terms of the densities of condensates  $n_{\pm}$  and their time-independent phases  $\phi_{\pm}$  as

$$\psi_{\pm} = \sqrt{n_{\pm}} e^{i\phi_{\pm}} f(x), \quad (113)$$

where  $f(x) = \sqrt{2} \cos \frac{\pi x}{d}$  is the transverse wave function corresponding to the ground state of a magnon. The total wave function is

$$\psi(\mathbf{r}) = \psi_+ e^{i\mathbf{Q}\mathbf{r}} + \psi_- e^{-i\mathbf{Q}\mathbf{r}} = [\sqrt{n_+} e^{i(Qz+\phi_+)} + \sqrt{n_-} e^{i(-Qz+\phi_-)}] f(x). \quad (114)$$

Introducing notation  $n = n_+ + n_-$  for the total density of condensate and  $\Phi(z) = 2Qz + \phi_+ - \phi_-$  for the phase difference of the two condensates, we find the square of modulus of the wave function:

$$|\psi(\mathbf{r})|^2 = [n + 2\sqrt{n_+ n_-} \cos \Phi(z)] f^2(x). \quad (115)$$

The square of gradient of the wave function is

$$|\nabla\psi|^2 = Q^2 [n - 2\sqrt{n_+ n_-} \cos \Phi(z)] f^2(x) + [n + 2\sqrt{n_+ n_-} \cos \Phi(z)] \left(\frac{df}{dx}\right)^2. \quad (116)$$

The fourth order exchange Hamiltonian contains two terms  $-|\psi|^2 |\nabla\psi|^2$  and  $\frac{1}{2} (\nabla |\psi|^2)^2$ . Assuming that densities of condensates  $n_{\pm}$  and their phases  $\phi_{\pm}$  vary in plane on the distances much larger than period of density oscillation  $L = 2\pi/Q$ , the density of interaction energy of condensates is equal to the exact value of interaction energy averaged over period of oscillation  $L$  integrated over the transverse coordinate  $x$ . For thick films the terms in  $\nabla\psi$  and  $\nabla |\psi|^2$  containing derivatives  $\frac{df}{dx}$  can be neglected in comparison with the terms containing derivatives over  $z$  or equivalently the value  $Q$  since  $Qd \gg 1$ . Performing simple operations of averaging and integration for exchange interaction we find:

$$\overline{\frac{H_{ex4}}{V}} = -\frac{3\mu_B^2 \ell^2}{16} Q^2 (n^2 - 6n_+ n_-) \quad (117)$$

Analyzing in similar way the interaction energy generated by dipolar Hamiltonian of the 4-th order, we should find the average of the integrand in the third equation (108). To make it, we will use the identity:

$$\frac{1}{|\mathbf{r} - \mathbf{r}'|} = \frac{1}{\pi} \iint_{-\infty}^{\infty} dq_y dq_z e^{i\mathbf{q}_{\parallel}(\mathbf{r}_{\parallel} - \mathbf{r}'_{\parallel})} G_{q_{\parallel}}(x - x'), \quad (118)$$

where the subscript  $\parallel$  at a vector means that it is parallel to the surfaces of the film, i.e., they have only  $y$  and  $z$ -components; we remind that the 1-dimensional Green function of the Helmholtz equation  $G_q(x)$  is defined by eq. (29). The proof of the identity (118) is given in the Appendix [1/r-G-identity]. Thus, the dipolar Hamiltonian of the 4-th order can be rewritten as follows:

$$\begin{aligned} H_{d4} = & \frac{\mu_B^2}{2\pi} \iiint dV dV' d^2 q_{\parallel} e^{i\mathbf{q}_{\parallel}(\mathbf{r}_{\parallel} - \mathbf{r}'_{\parallel})} \\ & \left[ |\psi|^2 |\psi'|^2 \partial_z \partial'_z - \frac{1}{8} (|\psi|^2 + |\psi'|^2) \right] \times \\ & (\psi \partial_- + \psi^* \partial_+) (\psi' \partial'_- + \psi'^* \partial'_+) G_{q_{\parallel}}(x - x') \end{aligned} \quad (119)$$

Note that we symmetrized the integrand over the variables  $\mathbf{r}$  and  $\mathbf{r}'$ . Except of the exponential function  $e^{i\mathbf{q}_{\parallel}(\mathbf{r}_{\parallel} - \mathbf{r}'_{\parallel})}$  the integrand does not depend of  $y$  and  $y'$ . Therefore the integration over  $y'$  gives  $2\pi\delta(q_y)$ . The partial derivatives  $\partial_{\pm} = \partial_x \pm iq_y$  become equal each to other and equal to  $\partial_x$ . The magnitude of derivatives  $\partial_z, \partial_{z'}$  is equal to  $Q$ , whereas the magnitude of the derivatives  $\partial_x, \partial_{x'}$  is equal to  $2\pi/d$ . For thick films  $Q \gg 1/d$ , therefore, the first term in the square brackets of this equation dominates. In this approximation we find

$$\begin{aligned} H_{d4} = & \mu_B^2 \int dV \int_{-d/2}^{d/2} dx' \int_{-\infty}^{\infty} dz' \int_{-\infty}^{\infty} dq_z \\ & [n + 2\sqrt{n_+ n_-} \cos \Phi(z)] [n + 2\sqrt{n_+ n_-} \cos \Phi(z')] \\ & [f(x) f(x')]^2 q_z^2 e^{iq_z(z-z')} G_{|q_z|}(x - x'). \end{aligned} \quad (120)$$

Since the integrand does not depend on  $y$ , the integration over this variable gives the linear size of sample  $L_y$ . Let us make change of variables  $Z = \frac{z+z'}{2}, \zeta = z - z'$ . The Jacobian of this transformation is 1. The only term

in the product of two square brackets in eq. (120) that together with exponential factor  $e^{iq_z(z-z')}$  gives non-zero average is  $4n_+n_- \cos \Phi(z) \cos \Phi(z') = 2n_+n_- [\cos(\Phi(z) + \Phi(z')) + \cos(\Phi(z) - \Phi(z'))]$ . From these two terms only the second gives nonzero average over  $z$ :

$$\int_{-\infty}^{\infty} d\zeta e^{iq_z\zeta} 2 \cos(2Q\zeta) = 2\pi [\delta(q_z - 2Q) + \delta(q_z + 2Q)] \quad (121)$$

This result allows us to perform also integration over  $q_z$ . Besides of that the integrand does not depend on  $Z$  and integration over this variable gives the linear size  $L_z$ . These integrations strongly simplify the expression for  $H_{d4}$ :

$$\overline{H_{d4}} = 4\pi\mu_B^2 L_y L_z Q n_+ n_- \iint_{-d/2}^{d/2} f^2(x) f^2(x') e^{-2Q|x-x'|} dx dx' \quad (122)$$

The calculation of the double integral in eq. (122) is elementary and gives:

$$\begin{aligned} & \iint_{-d/2}^{d/2} f^2(x) f^2(x') e^{-2Q|x-x'|} dx dx' \\ &= -\frac{-3d^5 Q^5 - 5\pi^2 d^3 Q^3 + \pi^4 (-2dQ - e^{-2dQ} + 1)}{2Q^2(d^2 Q^2 + \pi^2)^2}, \end{aligned} \quad (123)$$

In the limit of thick film  $Qd \gg 1$  the leading term is equal to  $3d/2Q$ . This dependence of the integral in (123) on parameters as  $d/Q$  could be predicted without detailed calculation since the exponent  $e^{-Q|x-x'|}$  cut in the square of integration a band of the width  $\sim 1/Q$  along the diagonal, whereas the average value of  $f^2$  is 1. However, strong fluctuations of  $f^2$  from 0 to 1 with period  $1/8$  of the diagonal requires explicit calculation to get exact numerical coefficient at the leading term:

$$\frac{\overline{H_{d4}}}{V} = 6\pi\mu_B^2 n_+ n_- \quad (124)$$

Thus, we have found the density of interaction energy between condensates of different minima (the inter-minima interaction). It can be written as

$$U_{4int} = B n_+ n_- \quad (125)$$

with  $B = 6\pi\mu_B^2 > 0$ . It is repulsion. Note that the terms of the same form in the exchange interaction energy (117) has coefficient  $B$  which differs from dipolar value by a factor  $\sim Q^2 \ell^2 \sim \ell/d \ll 1$  that can be neglected.

Another term that enters  $\overline{H_{ex4}}/V$  but is absent in  $\overline{H_{d4}}/V$  is interaction of the condensate magnons within one minimum

$$U_{4inn} = \frac{A}{2} (n_+^2 + n_-^2) \quad (126)$$

with  $A = -\frac{3}{8}\mu_B^2 Q^2 \ell^2$ . Thus, the interaction within one minimum is attraction. The magnitude  $|A|$  is much smaller than  $B$ :  $|A|/B = \frac{\pi^{1/2} \ell}{2^{7/2} d}$ . For YIG film  $5\mu\text{m}$  thick at room temperature  $|A|/B = 0.012$ .

#### 4.2.4 Quasi-equilibrium state.

In the experiment by Demokritov *et al.* [12] the low energy magnons in the YIG film were generated by a microstrip resonator. A photon of frequency  $\omega_{res}$  emitted by the resonator decays into two magnons with practically opposite momenta and frequency  $\omega_p = \omega_{res}/2$  (in classical electrodynamics this process is called parametric resonance or parametric pumping). The resonator frequency is chosen to be less than  $4\Delta/\hbar$ , where  $\Delta \approx 2\mu_B\mathcal{H}$  is the minimal energy of magnons (gap in the spectrum). Then the decays of pumped magnons are forbidden, whereas their collisions with other low energy magnons remain possible. These collisions establish the equilibrium. The relaxation time  $\tau_r$  is just the time between collisions. An important role is played by the processes of the Cherenkov radiation of a low-energy magnon by a thermal magnon and inverse process of the absorption of the low-energy magnon by a thermal magnon. These processes determine the lifetime of low-energy magnons  $\tau_l$ . In YIG at room temperature  $\tau_r \ll \tau_l$ . It means that during the relaxation the number of magnons is conserved and they go to equilibrium with the finite chemical potential  $\mu$ . The role of pumping is to restore the stationary number of magnons in exchange of absorbed ones. We will call such a stationary state quasi-equilibrium.

Let us consider the balance of magnons following Bun'kov and Volovik.[21] The occupation number of a low-energy magnon with energy  $\varepsilon$  in the quasi-equilibrium state is  $n(\varepsilon) = \frac{T}{\varepsilon - \mu}$ . The occupation number of the magnon with the same energy in equilibrium without pumping is  $n_0(\varepsilon) = \frac{T}{\varepsilon}$ . The total density  $n_{pm}(T, \mu)$  of pumped magnons is

$$n_{pm}(T, \mu) = \int_0^{\infty} [n(\varepsilon) - n_0(\varepsilon)] \bar{g}(\varepsilon) d\varepsilon, \quad (127)$$

where  $\bar{g}(\varepsilon)$  is the magnon density of state per unit volume. It can be rewritten as

$$n_{pm}(T, \mu) = \int_0^{\infty} \frac{T\mu}{\varepsilon(\varepsilon - \mu)} \bar{g}(\varepsilon) d\varepsilon. \quad (128)$$

The density of magnons pumped per unit time is determined by the pumped power  $W$  per unit volume as  $\frac{2W}{\hbar\omega_{res}}$ . In a stationary state it must be equal to the density of pumped magnons that disappear per unit time  $\frac{n_{pm}}{\tau_l}$ . Thus, the established density of pumped magnons is

$$n_{pm} = \frac{2W}{\hbar\omega_{res}} \tau_l. \quad (129)$$

Replacing  $n_{pm}$  by the integral in the r.-h. side of eq. (128), we obtain equation relating the chemical potential  $\mu$  to the pumped power  $W$ . This equation implies that  $\mu$  grows monotonically with  $W$  growing. At a critical value of the pumped



power

$$W^{(c)} = \frac{\hbar\omega_{res}}{2\pi_l} \int_{\Delta}^{\infty} \frac{T\Delta}{\varepsilon(\varepsilon - \Delta)} \bar{g}(\varepsilon) d\varepsilon, \quad (130)$$

chemical potential reaches its maximum possible value  $\mu_{\max} = \Delta$  and the density of pumped magnons reaches its critical value

$$n_{pm}^{(c)} = \int_{\Delta}^{\infty} \frac{T\Delta}{\varepsilon(\varepsilon - \Delta)} \bar{g}(\varepsilon) d\varepsilon. \quad (131)$$

Chemical potential cannot grow more since at  $\mu > \Delta$ , the occupation number of magnons with energy between  $\Delta$  and  $\mu$  would be negative that is nonsense. Therefore, at  $W > W^{(c)}$  the chemical potential remains unchanged  $\mu = \Delta$ . The excessive magnons go to the state with minimal energy  $\Delta$  and form the BEC. The condensate density is

$$n_c = \frac{2(W - W^{(c)})}{\hbar\omega_{res}} \pi_l. \quad (132)$$

All these calculations assumed that the integrals are converging. There are two possible sources of divergence: large energies  $\varepsilon \rightarrow \infty$  and  $\varepsilon$  close to  $\Delta$  for  $W \geq W^{(c)}$ . For large  $\varepsilon$  the exchange interaction dominates, the magnon energy is quadratic function of momentum and  $\bar{g}(\varepsilon) \propto \sqrt{\varepsilon}$ , whereas the denominator of integrand in eq. (128) asymptotically approaches  $\varepsilon^2$ . Thus, the integral converges at  $\varepsilon \rightarrow \infty$ . This result physically means that the pumped magnons after relaxation remain in the range of low energy  $\sim \Delta$ . Paradoxically their energy escapes into the range  $\iota \sim T$ . Indeed, the pumped energy is

$$E_{pm} = \int_0^{\infty} \frac{T\mu}{\varepsilon(\varepsilon - \mu)} \varepsilon \bar{g}(\varepsilon) d\varepsilon. \quad (133)$$

This integral diverges at  $\varepsilon \rightarrow \infty$ . It happens because we applied low-energy Rayleigh-Jeans approximation  $n(\varepsilon) = \frac{T}{\varepsilon - \mu}$ ,  $n_0(\varepsilon) = \frac{T}{\varepsilon}$  for the occupation numbers of magnons, which at high energy must be replaced by the Planck-Bose-Einstein distribution  $n(\varepsilon) = (\exp \frac{\varepsilon - \mu}{T} - 1)^{-1}$ ,  $n_0(\varepsilon) = (\exp \frac{\varepsilon}{T} - 1)^{-1}$ . Thus, the integral (133) is cut-off at  $\varepsilon \sim T$ . Neglecting  $\mu$  in denominator of integrand, we find the rough estimate of the pumped energy per unit volume  $\mu T^{3/2} / [(\mu_B M)^{3/2} \ell^3]$  that corresponds to the change of the magnons temperature by  $\delta T \approx \Delta / k_B$ . For YIG film in external magnetic field  $\mathcal{H} = 600\text{Oe}$  and at room temperature, the resulting increase of temperature is about  $0.04K$ .

The convergence at the points of minimum energy  $\varepsilon = \Delta$  follows from the fact that, in the continuous limit, they are isolated points in 3-dimensional space. Therefore, the density of states near each minimum goes to zero as  $\sqrt{\varepsilon - \Delta}$ .

#### 4.2.5 Spontaneous violation of the reflection symmetry in the quasi-equilibrium state.

In the state of quasi-equilibrium its energy (more accurately its Helmholtz free energy) must be minimum. At fixed temperature and volume, the free energy has minimum when the occupation numbers obey the Bose-Einstein law and excessive magnons occupy the state with minimal energy  $\Delta$ . In ferromagnetic films there are two such states. Therefore, the ground state of the ideal magnon gas is highly degenerate: the condensate energy  $E_{id} = Vn_c\Delta$  depends only on the total number of magnons in condensate  $N_c = Vn_c = N_+ + N_-$  and does not depend on how these magnons are distributed between two minima. This  $N_c + 1$ -fold degeneration is lifted by magnons interaction.[20]

As it was derived in the subsection,4.2.3 the 4-th order interaction density of energy is

$$U_4 = \frac{A}{2} (n_+^2 + n_-^2) + Bn_+n_-, \quad (134)$$

with  $A < 0$  and  $B > 0$  for thick films. The interaction energy  $U_4$  has minimum equal to  $U_4 = -\frac{A}{2}n^2$  either at  $n_+ = n, n_- = 0$  or at  $n_+ = 0, n_- = n$ . In both cases the symmetry with respect to reflection in the plane  $z = 0$  combined with the time reversal is violated. Unfortunately such a most asymmetric state contradicts to the experiment and to a more sophisticated theory.

Let us start with the experiment. In 2012 in the work by P. Novik-Boltyk *et al.* [22] the Münster experimental team led by S. Demokritov discovered a stripe interference structure of the magnetization  $M_z$  in the YIG sample (see the interference picture in Fig. 11.) It can be interpreted as the measurement of

$$|\psi|^2 = |\sqrt{n_+}e^{iQz+\phi_+} + \sqrt{n_-}e^{-iQz+\phi_-}|^2 = n + 2\sqrt{n_+n_-} \cos(2Qz + \phi_+ - \phi_-).$$

This equation clearly shows that the interference picture can be observed only if both  $n_+$  and  $n_-$  are not zero. In order to explain this result, F. Li, W. Saslow and V. Pokrovsky[23] proposed to consider the additional term in the 4-th order interaction Hamiltonian of purely dipolar origin of the form

$$\frac{C}{2} [(\psi_+^* \psi_+^2 \psi_- + c.c.) + (+ \leftrightarrow -)] \quad (135)$$

where the abbreviation *c.c.* stays for complex conjugate,  $C$  is a real constants whose magnitude in terms of parameters is of the same order as  $|A|$ , however the numerical constant in  $C$  is by a factor  $1/2\pi^3 \approx 0.016$  smaller. This term is contained in the earlier neglected terms of the 4-th order dipolar interaction containing derivatives over  $x$ . The real processes associated with this term would be decay of one condensate magnon in three and inverse process of merging three condensate magnon in one. All such processes are forbidden by the energy conservation. However, they determine additional (anomalous) 4-order interaction energy:

$$\frac{H_{4an}}{V} = Cn\sqrt{n_+n_-} \cos(\phi_+ + \phi_-) \quad (136)$$

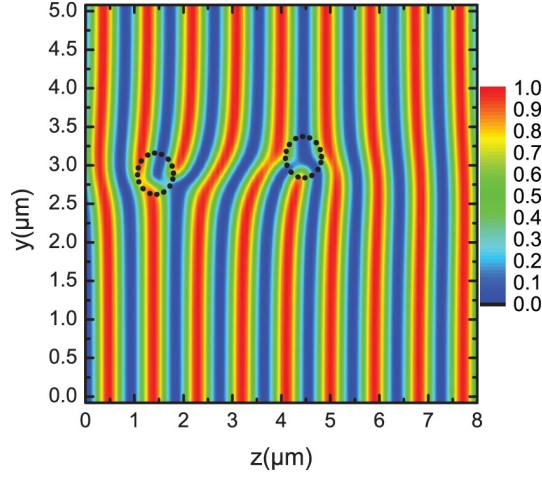


Figure 11: Measurement of the BLS intensity. Dashed circles indicate the positions of two defects causing an appearance of two vortices of positive circulation in different components of the condensate. The vortices show themselves as forks in the interference pattern. Reprinted by permission from Macmillan Publishers Ltd: Scientific Reports [22], Copyright 2012.

Note that this energy depends on a different combination of phases  $\phi_+ + \phi_-$  than the Goldstone phase  $\phi_+ - \phi_-$  whose variation does not change energy. The minimum energy is reached at  $\phi_+ + \phi_- = \pi$  or  $0$  depending on the sign of the coefficient  $C$ . On the line  $C = 0$  the transition from  $0-$  to  $\pi-$  phase or vice versa proceeds. In both these phases the minimum anomalous interaction energy is negative:

$$\min \left( \frac{H_{4an}}{V} \right) = -|C| n \sqrt{n_+ n_-}. \quad (137)$$

Thus, the total 4-th order interaction energy acquires the form:

$$U_4 \equiv \frac{H_4}{V} = \frac{A}{2} (n_+^2 + n_-^2) + B n_+ n_- - |C| n \sqrt{n_+ n_-} \quad (138)$$

Its minimization at a fixed  $n$  gives:

$$\frac{n}{\sqrt{n_+ n_-}} = \frac{2(B-A)}{|C|}. \quad (139)$$

Let us denote  $R = \frac{B-A}{|C|} + \sqrt{\left(\frac{B-A}{|C|}\right)^2 - 1}$  and  $\Theta = \frac{|C|}{2(B-A)R}$ . The value  $R$  is very big, whereas the value  $\Theta \approx \frac{1}{4R^2}$  is very small. The two solutions of this equation are either

$$\begin{aligned} n_+ &= (1 - \Theta) n; \\ n_- &= \Theta n, \end{aligned} \quad (140)$$

or  $n_+$  and  $n_-$  interchange. In each solution one of two condensate densities is much larger than another, but the smaller one turns into zero only if  $C = 0$ . The total interaction energy in this phase is

$$U_4 = n^2 \left[ \frac{A}{2} + \frac{|C|}{2R} (1 - \Theta) - |C| \sqrt{\Theta(1 - \Theta)} \right] \quad (141)$$

$$\approx n^2 \left( \frac{A}{2} - \frac{C^2}{4B} \right) < 0$$

#### 4.2.6 Instability of homogeneous asymmetric phase.

We have found that the homogeneous phase with the violated reflection symmetry has negative interaction energy proportional to  $n^2$ . It means that the interaction energy decreases when the volume occupied by the condensate decreases. In the weakly non-ideal attractive Bose-gas of  $N$  particles with the coupling constant  $g < 0$  and mass  $m$  of particle this tendency leads to the mechanical instability of the gas and its collapse at a critical value of number of particles  $N_c$ . At this value the isothermal compressibility  $\kappa_T = -\frac{1}{V} \left( \frac{\partial V}{\partial P} \right)_T$  is zero and at  $N > N_c$  becomes negative. Due to quantum uncertainty, the kinetic energy per particle can be written as  $K/N = \frac{\hbar^2}{2mV^{2/3}}$ , whereas the interaction energy is  $U = \frac{gN^2}{2V}$ . Thus, the total energy is

$$E(N, V) = N \frac{\hbar^2}{2mV^{2/3}} + \frac{gN^2}{2V}. \quad (142)$$

The pressure is

$$P = -\frac{\partial E}{\partial V} = \frac{\hbar^2 N}{3mV^{5/3}} + \frac{gN^2}{2V^2} \quad (143)$$

and the compressibility is

$$\kappa_T = \frac{5\hbar^2 N}{9mV^{5/3}} + \frac{gN^2}{V^2} \quad (144)$$

Equation  $\kappa_T = 0$  determines the critical number of particles  $N_c = -\frac{5\hbar^2 V^{1/3}}{9mg}$ . At  $N > N_c$ , the compressibility is negative and the gas becomes mechanically unstable. It starts to contract. Since this process proceeds simultaneously in the total volume occupied by the gas, the process will stop when the volume will be divided into  $N/N_c$  cells each containing  $N_c$  particles and isolated each from other. The volume of such a cell is  $v = VN_c/N$ , therefore the critical number in a cell is different than the critical number in the entire volume. It should be found from equation  $N_c = \frac{5\hbar^2}{9m|g|} \left( \frac{VN_c}{N} \right)^{1/3}$ . It is convenient to express the coupling constant  $g$  in terms of the Born scattering length  $a_s$  as  $g = \frac{\hbar^2}{m} a_s$ . Then  $N_c = \frac{5^{3/2}}{27} \frac{1}{n^{1/6} |a_s|^{1/2}}$ , where  $n = N/V$  is the average density of particles. For a weakly interacting Bose gas  $n^{1/3} |a_s| \ll 1$ . Therefore  $N_c \gg 1$ . The collapse was observed in cooled gases of alkali atoms  $^7\text{Li}$  [24] and  $^{85}\text{Rb}$  [25]. At finite temperature the pressure from excitations must be included. It changes the critical values for starting the collapse, but the collapse persists. Gases of

cooled attracting alkali atoms after the collapse flew out the magnetic or laser trap. Our calculations relate to the Bose gas of quasiparticles that cannot avoid the system in which they exist like excitons in semiconductors or spin waves in magnets.

Theoretical predictions for starting parameters of collapse in weakly attracting Bose gas at finite temperature were made by Mueller and Baym.[26] Dynamic approach to the same problem was developed by Pitaevskii. [27]

For the magnon condensation in a ferromagnetic film, the problem is effectively two-dimensional. It is because the minimum of energy corresponds to the transverse standing wave, period of which fits between surfaces of the film. The effective masses are strongly anisotropic (see subsection 3.5.3). The curve of constant kinetic energy is the ellipsis  $\frac{\hbar^2 k_y^2}{2m_y} + \frac{\hbar^2 k_z^2}{2m_z} = K$ . Therefore we expect that the collapsed magnon condensate will be limited by an ellipsis with semi-axes  $R_y, R_z$  whose ratio is  $R_y/R_z = \sqrt{m_z/m_y}$ . Then the kinetic energy of collapsed condensate can be estimated as

$$K = N \left( \frac{\hbar^2}{2m_y R_y^2} + \frac{\hbar^2}{2m_z R_z^2} \right) = \frac{N\hbar^2}{\sqrt{m_y m_z} R_y R_z}, \quad (145)$$

whereas the condensate potential energy is

$$U = \frac{gN^2}{2\pi R_y R_z d}. \quad (146)$$

The pressure at zero temperature is

$$P = \frac{N}{V^2} \left( \frac{\pi\hbar^2 d}{\sqrt{m_y m_z}} + \frac{g}{2} N \right), \quad (147)$$

where  $V = \pi R_y R_z d$  is the volume of the condensate cloud. The compressibility of the magnon gas in the film differs from the pressure only by numerical factor 2. Thus, the pressure and compressibility simultaneously become zero when  $N$  reaches a critical value

$$N_c = -\frac{2\pi\hbar^2 d}{\sqrt{m_y m_z} g} = \frac{2\pi d}{|a_s|}. \quad (148)$$

The film will be divided into  $N/N_c$  almost isolated cells each containing  $N_c$  magnons. Let the cell be a rectangle with the sides  $R_y, R_z$ . If  $A$  is the area of the sample, then the area of a cell is  $R_y R_z = \frac{AN_c}{N}$ . From this equation and requirement  $R_y/R_z = \sqrt{m_z/m_y}$  we find  $R_y = \left(\frac{m_z}{m_y}\right)^{1/4} \sqrt{\frac{AN_c}{N}}$ ;  $R_z = \left(\frac{m_y}{m_z}\right)^{1/4} \sqrt{\frac{AN_c}{N}}$ . According to eq. (148), this result can be rewritten as

$$R_y = \left(\frac{m_z}{m_y}\right) \sqrt{\frac{2\pi}{n|a_s|}}; R_z = \left(\frac{m_y}{m_z}\right)^{1/4} \sqrt{\frac{2\pi}{n|a_s|}}, \quad (149)$$

where  $n = N/(Ad)$  is the average density of magnons. The collapse destroys the homogeneous coherent condensate transforming it into a set of isolated islands.

For YIG with  $n = 10^{18} \text{cm}^{-3}$  we find  $N_c \approx 1.14 \times 10^5$ ,  $R_y \approx 1.16 \times 10^{-6} \text{cm}$ ;  $R_z \approx 0.58 \times 10^{-7} \text{cm}$ . There is no experimental evidence of the cell structure in YIG films.

### 4.3 New experiments and our new theoretical ideas about slow inter-minima relaxation and laser effects.

Two recent articles by the Münster University experimental team led by S.O. Demokritov [28, 29] revealed several important facts about the Bose-Einstein condensation of magnons (BECM) under permanent pumping first discovered in 2006 [12]. Existing theories of this phenomenon predict an attractive interaction between magnons [30, 31, 23] and a strong spontaneous violation of the reflection symmetry [23]. However these theories implicitly assumed that all relaxation processes were fast compared to the lifetime of magnons, whereas one of them, the relaxation between two energy minima, is slow.

We predict the properties of the stationary state of the magnon gas with condensate, that is far from equilibrium with respect to variables responsible for inter-minima coherence. The momentum-flip relaxation time is no less than 1 hour, which exceeds even the time of the experiment without considering the lifetime. It means that the equilibrium between condensates in different minima is never reached. As a result, the condensates' stationary state is far from equilibrium. In this regard, it is analogous to the laser stationary state, and, like the laser, the magnon condensate state can produce coherent magnon radiation [32, 33].

The very slow inter-minima relaxation implies that the appearance of the stationary condensate in a ferromagnetic film is a dynamic phase transition. Since the inter-minima equilibrium is not established, the pumping, which is symmetric with respect to the two minima, creates equal numbers of magnons in the two condensates  $n_+ = n_- = n_c/2$ . Therefore, the inter-minima repulsion energy  $Bn_+n_- = Bn_c^2/4$  strongly exceeds the magnitude of in-minimum attraction  $\frac{|A|}{2}(n_+^2 + n_-^2) = |A|n_c^2/4$ . This consideration explains why experimenters observe repulsion of magnons in the stationary state with the condensate. With a somewhat more sophisticated point of view, the mirror symmetry of the pumping does not necessarily lead to the same symmetry of the condensate. In principle, dynamic violation of mirror symmetry is possible. But in this case, there is no reason why it should be strong. This issue requires further theoretical investigation.

It is difficult to avoid a slight asymmetry of the device in real-world experiments, which favors a slightly asymmetric stationary state. Such a device asymmetry could explain the asymmetry observed in the experiment II by Borisenko et al. If the asymmetry is relatively small, then in eq. (139) the term  $Bn_+n_-$  is dominant and positive, but it completely conceals the possibility of dynamic spontaneous violation of the reflection symmetry.

Because the inter-minima equilibrium is not established, the consistent theory of the stationary state with condensate necessitates solving the Boltzmann

kinetic equation for magnons and the Gross-Pitaevskii equations for the two condensates. It can be accomplished using either a variational technique based on the idea of maximal entropy production or by solving a problem with proper initial conditions that asymptotically approaches a stationary state.

This kinetic approach may help to bridge another gap between the existing theories [21, 20] and experiment [32, 33]. The theory proves that the pumped magnons are accumulated in the low-energy region assuming the temperature of accumulated magnons to be the same as initial temperature of the system (room temperature). The temperature of low energy magnons is approximately three times higher, according to experimental data. If the temperature is a slow-varying function of energy (momentum) that saturates to the system's room temperature at some intermediate energy between  $\mu_B H$  and the room temperature, the controversy may be resolved.

## Acknowledgments.

We are thankful to T. Nattermann, W.M. Saslow, Fuxiang Li, Chen Sun together with whom were obtained many results mentioned in this article. Our gratefulness is due to S.O. Demokritov and participants of his experimental team V. E. Demidov, I. Borisenko, B. Divinskii, P. Novik-Boltyk for many useful discussions of the experimental results and cooperation. We thank J. Ketterson and J. Lim for explanation of their experiment and discussion of its results. We are indebted to B. Hillebrands, A. Serga and D. Bozhko for discussion of their experiments. Many theoretical problems were discussed with A.N. Slavin, V.S. L'vov and G. E. Volovik, who also informed us on a vast literature on the subject. Our thanks to them. We remember thankfully the discussion with deceased L.P. Pitaevskii on the instability of attractive Bose condensate.

## Appendix 1. Motion of minima.

The dependence of frequency on wave vector is determined by equation (82) of the main text. For the reader's convenience we reproduce it:

$$\omega^2 = \mu_B^2 \mathcal{H}^2 (1 + k^2) \left( 1 + k^2 + \chi - \chi \frac{k_z^2}{k^2} \right) \quad (150)$$

Here  $k^2 = k_{\parallel}^2 + k_x^2$ , where  $k_x$  is a positive quantized transverse component of wave vector. Generally to find minimum of frequency for a given mode with fixed quantum numbers and direction of propagation, it is necessary to take in account the dependence of quantized  $k_x$  on  $k_{\parallel}$ . This dependence can be neglected in thick films with  $d \gg 1$ . Indeed according to the main text, quantized values of  $k_x$  are equal to  $k_{x,\nu,n} = \frac{2\pi n}{d} + \mu_{\nu,n}$ . Here  $\mu_{\nu,n} = \frac{2}{d} \arctan f_{\nu,n}(k_{\parallel})$ , where  $f_{\nu,n}(k_{\parallel})$  is a smooth function. According to this definition,  $\mu_{\nu,n}$  varies in the limits  $(-\frac{\pi}{d}, \frac{\pi}{d})$  when  $k_{\parallel}$  changes at least by  $1/\sqrt{d}$ . Therefore, the derivative  $\frac{dk_x}{dk_{\parallel}} \lesssim \frac{1}{\sqrt{d}} \ll 1$  and the values  $k_{\parallel}$  and  $k_x$  can be considered as independent. In this approximation

the value of parallel wave vector  $k_{\parallel 0}$  at which frequency has minimum can be found from equation:

$$\frac{\partial \omega^2}{\partial (k_{\parallel}^2)} = 2k^2 + 2 + \chi \sin^2 \theta - \frac{\chi k_x^2 \cos^2 \theta}{k^4} = 0 \quad (151)$$

At small  $k_x$  i.e. at  $n \ll d/2\pi$ , the value  $k^2$  satisfying eq. (151) is also small and equal to

$$k_0^2 \approx k_{\parallel 0}^2 \approx \sqrt{\frac{\chi}{2 + \chi \sin^2 \theta}} k_x \cos \theta \quad (152)$$

It is however much larger than  $k_x^2$ . The value of frequency in minimum is  $\omega_{min} \approx \sqrt{1 + \chi \sin^2 \theta}$ . The equation for  $k_0^2$  valid in the range of larger  $k_x$  comparable with 1 can be found by the following scaling transformation:

$$k_0^2 = \frac{2 + \chi \sin^2 \theta}{2} w(\xi); \quad \xi = \frac{4\chi k_x^2 \cos^2 \theta}{(2 + \chi \sin^2 \theta)^3}, \quad (153)$$

where function  $w(\xi)$  obeys cubic equation:

$$w^3 + w^2 = \xi \quad (154)$$

At small  $\xi$ , this equation gives the result (152). This equation shows that at small  $k_x$ , the wave vector corresponding to minimal frequency  $k_{\parallel 0}$  grows with  $k_x$ . To study the motion of minimum in a broader interval of  $k_x$  it is useful to look at the derivative  $\frac{dk_{\parallel 0}^2}{d(k_x^2)}$ . According to eq. (151), it can be expressed as follows:

$$\frac{dk_{\parallel 0}^2}{d(k_x^2)} = -\frac{\frac{\partial^2 \omega^2}{\partial (k_{\parallel}^2) \partial (k_x^2)}}{\left(\frac{\partial^2 \omega^2}{\partial (k_{\parallel}^2)}\right)^2} \quad (155)$$

From this equation it follows that maximal value of  $k_{\parallel 0}$  can be found from equation:

$$\frac{\partial^2 \omega^2}{\partial (k_{\parallel}^2) \partial (k_x^2)} = 2 - \chi \frac{\cos^2 \theta}{k^4} + 2\chi \frac{k_x^2 \cos^2 \theta}{k^6} = 0 \quad (156)$$

It is cubic equation for  $k^2$ . It must be solved together with equation of frequency minimum (151). Eliminating  $k_x^2$  from these two equations, we arrive at a closed equation for  $k^2$ :

$$6k^6 + 2(2 + \chi \sin^2 \theta) k^4 - \chi \cos^2 \theta k^2 = 0 \quad (157)$$

Dividing this equation by  $k^2 \neq 0$ , we obtain a quadratic equation for  $k^2$ , whose solution reads:

$$k_m^2 = \frac{\sqrt{(2 + \chi \sin^2 \theta)^2 + 6\chi \cos^2 \theta} - (2 + \chi \sin^2 \theta)}{6} \quad (158)$$



The value of  $k_x^2$  corresponding to maximal value of  $k_{\parallel 0}$  can be found by eliminating  $k^6$  from eqs. (151,157). It reads:

$$(k_x^2)_m = \frac{1}{3\chi \cos^2 \theta} [(2 + \chi \sin^2 \theta) k_m^4 + \chi \cos^2 \theta k_m^2] \quad (159)$$

The maximal value of  $k_{\parallel 0}^2$  is equal to

$$(k_{\parallel 0}^2)_{\max} = k_m^2 - (k_x^2)_m = \frac{2}{3}k_m^2 - \frac{(2 + \chi \sin^2 \theta) k_m^4}{3\chi \cos^2 \theta}$$

At further increase of  $k_x$ , the position of minimum  $k_{\parallel 0}$  decreases and finally becomes zero. At this point,  $k^2 = k_x^2$  and eq. (151) turns into quadratic equation for  $k_x^2$ . Its solution reads:

$$(k_x^2)_f = \frac{\sqrt{(2 + \chi \sin^2 \theta)^2 + 8\chi \cos^2 \theta} - (2 + \chi \sin^2 \theta)}{4}$$

At this value of  $k_x$ , minimum merges with a local maximum at  $k_{\parallel} = 0$ . At larger values of  $k_x$ , the only minimum of frequency is at  $k_{\parallel} = 0$ .

## Appendix 2. Hamiltonian of the 4-th order.

. According to the subsection 4.2.2, the 4-th order Hamiltonian is:

$$H_4 = \sum_{i,k,l=1}^4 \sum_{\mathbf{q}_i n_k \rho_l} I_{4\mathbf{q}_1 n_1, \mathbf{q}_2 n_2, \mathbf{q}_3 n_3, \mathbf{q}_4 n_4}^{(\rho_1 \rho_2 \rho_3 \rho_4)} \left[ \prod_{j=1}^4 \eta_{\mathbf{q}_j n_j}^{(\rho_j)} \right] \delta_{\mathbf{q}_1 + \mathbf{q}_2 + \mathbf{q}_3 + \mathbf{q}_4}, \quad (160)$$

where  $\eta_{\mathbf{q}n}^{(+)} = \eta_{\mathbf{q}n}$ ,  $\eta_{\mathbf{q}n}^{(-)} = \eta_{-\mathbf{q}n}^*$  and upper indices  $\rho_l$  ( $l = 1, 2, 3, 4$ ) take values  $+, -$  independently each from others. In terms of complex indices  $\gamma_i = (\rho_i \mathbf{q}_i n_i)$  the Hamiltonian  $H_4$  can be rewritten as

$$H_4 = \sum_{\gamma_i} I_{\gamma_1 \gamma_2 \gamma_3 \gamma_4} \eta_{\gamma_1} \eta_{\gamma_2} \eta_{\gamma_3} \eta_{\gamma_4} \delta_{\mathbf{q}_1 + \mathbf{q}_2 + \mathbf{q}_3 + \mathbf{q}_4} \quad (161)$$

Since the product of four  $\eta_j$  is symmetric at any permutation  $P$  of four  $j$ , it is possible to replace the initial coefficients  $I_{\gamma_1 \gamma_2 \gamma_3 \gamma_4}$  by the symmetrized coefficients

$$I_{\gamma_1 \gamma_2 \gamma_3 \gamma_4}^s = \frac{1}{24} \sum_P I_{\gamma_{P1} \gamma_{P2} \gamma_{P3} \gamma_{P4}}, \quad (162)$$

where  $Pj$  means the number appearing on  $j$ -th place at permutation  $P$ . For example, for the permutation  $1, 2, 3, 4 \rightarrow 4, 3, 2, 1$  one finds  $P1 = 4$ ,  $P2 = 3$ ,  $P3 = 2$ ,  $P4 = 1$ .

Let us now analyze what are constraints for symmetrized coefficients following from the fact that the energy is real. To make notations more compact

further we omit the subscript 4 and round brackets in upper part of initial coefficients. Then eq. (161) turns into

$$H_4 = \sum_{\mathbf{q}_k n_l \rho_m} I_{\mathbf{q}_1 n_1 \mathbf{q}_2 n_2 \mathbf{q}_3 n_3, \mathbf{q}_4 n_4}^{s \rho_1 \rho_2 \rho_3 \rho_4} \prod_{j=1}^4 \eta_{\mathbf{q}_j n_j}^{\rho_j}. \quad (163)$$

Since  $\eta_{\mathbf{q}_j n_j}^- = \left( \eta_{-\mathbf{q}_j n_j}^+ \right)^*$ , the energy is real if the following relations are satisfied:

$$I_{\mathbf{q}_1 n_1 \mathbf{q}_2 n_2 \mathbf{q}_3 n_3, \mathbf{q}_4 n_4}^{s-\rho_1-\rho_2-\rho_3-\rho_4} = \left( I_{-\mathbf{q}_1 n_1 -\mathbf{q}_2 n_2 -\mathbf{q}_3 n_3, -\mathbf{q}_4 n_4}^{s \rho_1 \rho_2 \rho_3 \rho_4} \right)^* \quad (164)$$

However, the initial non-symmetrized coefficients  $I_{\mathbf{q}_1 n_1 \mathbf{q}_2 n_2 \mathbf{q}_3 n_3, \mathbf{q}_4 n_4}^{\rho_1 \rho_2 \rho_3 \rho_4}$  calculated according to the rules formulated in the subsection 4.2.2. do not obey these relationships. Nevertheless, not all of them are independent. In this Appendix we derive the integral presentation for independent coefficients and find relations that allow to find the rest of them.

At fixed values  $\mathbf{q}_i, n_i; i = 1, 2, 3, 4$ , there are  $2^4 = 16$  different combinations of  $\rho_j = \pm$  that defines coefficients  $I_{\mathbf{q}_1 n_1 \mathbf{q}_2 n_2 \mathbf{q}_3 n_3, \mathbf{q}_4 n_4}^{\rho_1 \rho_2 \rho_3 \rho_4}$ . Each of them contains contributions from exchange  $I_e$  and dipolar  $I_d$  interactions, in total 32 coefficients. In each of them  $\rho_j$  take the same value + or - more than once. It allows to make the partial symmetrization over repeating indices. For a further compactification of notations we denote the pair  $j \equiv \mathbf{q}_j n_j$  and  $\bar{j} = -\mathbf{q}_j n_j; j = 1, 2, 3, 4$ . Then the resulting relationships for exchange coefficients are:

$$I_{e1234}^{----} = \left( I_{e4321}^{++++} \right)^* \quad (165)$$

$$I_{e1234}^{---+} = \left( I_{e2143}^{++--} \right)^* = \left( I_{e4321}^{-+++} \right)^* \quad (166)$$

$$I_{e1234}^{+---} = \left( I_{e2143}^{+-++} \right)^* = \left( I_{e4321}^{++++} \right)^* \quad (167)$$

$$I_{e1234}^{--+-} = \left( I_{e4321}^{+---} \right)^* = \left( I_{e2143}^{++++} \right)^* \quad (168)$$

$$I_{e1234}^{-+--} = \left( I_{e4321}^{++--} \right)^* = \left( I_{e2143}^{---+} \right)^* \quad (169)$$

$$I_{e1234}^{--++} = I_{e3412}^{++--} = I_{e3214}^{+-++} = I_{e1432}^{-+--} \quad (170)$$

Altogether there are 10 equations for 16 exchange coefficients. Thus, only 6 of them are independent. This 6 coefficients can be chosen as:

$$I_{e1234}^{++++} = \frac{\mu_B^2 \ell^2}{4A} \int_{-d/2}^{d/2} [(d_x u_1^*) v_2^* (d_x u_3^*) v_4^* + u_1^* (d_x v_2^*) u_3^* (d_x v_4^*) - \frac{1}{2} \left( \sum_{j=1}^4 \mathbf{q}_j^2 \right) u_1^* v_2^* u_3^* v_4^*] dx; \quad (171)$$

$$I_{e1234}^{++++} = -\frac{\mu_B^2 \ell^2}{4A} \int_{-d/2}^{d/2} [(d_x u_1^*) v_2^* (d_x u_3^*) u_4^* + u_1^* (d_x v_2^*) u_3^* (d_x u_4^*) - \frac{1}{2} \left( \sum_{j=1}^4 \mathbf{q}_j^2 \right) u_1^* v_2^* u_3^* u_4^*] dx; \quad (172)$$

$$I_{e1234}^{-++++} = -\frac{\mu_B^2 \ell^2}{4A} \int_{-d/2}^{d/2} [(d_x v_{\bar{1}}) v_2^* (d_x u_3^*) v_4^* + v_{\bar{1}} (d_x v_2^*) u_3^* (d_x v_4^*) - \frac{1}{2} \left( \sum_{j=1}^4 \mathbf{q}_j^2 \right) v_{\bar{1}} v_2^* u_3^* v_4^*] dx; \quad (173)$$

$$I_{e1234}^{+++-} = \frac{\mu_B^2 \ell^2}{4A} \int_{-d/2}^{d/2} [(d_x u_{\bar{1}}) v_2^* (d_x v_3) u_{\bar{4}} + u_{\bar{1}}^* (d_x v_2^*) v_3 (d_x u_{\bar{4}}) - \frac{1}{2} \left( \sum_{j=1}^4 \mathbf{q}_j^2 \right) u_{\bar{1}}^* v_2^* v_3 u_{\bar{4}}] dx; \quad (174)$$

$$I_{e1234}^{+-+-} = \frac{\mu_B^2 \ell^2}{4A} \int_{-d/2}^{d/2} [(d_x u_{\bar{1}}) u_{\bar{2}} (d_x u_3^*) u_{\bar{4}} + u_{\bar{1}}^* (d_x u_{\bar{2}}) u_3^* (d_x u_{\bar{4}}) - \frac{1}{2} \left( \sum_{j=1}^4 \mathbf{q}_j^2 \right) u_{\bar{1}}^* u_{\bar{2}} u_3^* u_{\bar{4}}] dx; \quad (175)$$

$$I_{e1234}^{-+--} = \frac{\mu_B^2 \ell^2}{4A} \int_{-d/2}^{d/2} [(d_x v_{\bar{1}}) v_2^* (d_x v_3) v_4^* + v_{\bar{1}} (d_x v_2^*) v_3 (d_x v_4^*) - \frac{1}{2} \left( \sum_{j=1}^4 \mathbf{q}_j^2 \right) v_{\bar{1}} v_2^* v_3 v_4^*] dx. \quad (176)$$

There only 8 relationships for the dipolar part of 4-th order Hamiltonian:

$$I_{d1,2,3,4}^{----} = \left( I_{d\bar{2},\bar{1},\bar{3},\bar{4}}^{++++} \right)^* \quad (177)$$

$$I_{d1,2,3,4}^{-+--} = \left( I_{d\bar{2},\bar{1},\bar{3},\bar{4}}^{-+++} \right)^* \quad (178)$$

$$I_{d1,2,3,4}^{+---} = \left( I_{d\bar{2},\bar{1},\bar{3},\bar{4}}^{+--+} \right)^* \quad (179)$$

$$I_{d1,2,3,4}^{--+-} = \left( I_{d\bar{2},\bar{1},\bar{3},\bar{4}}^{++-+} \right)^* \quad (180)$$

$$I_{d1,2,3,4}^{---+} = \left( I_{d\bar{2},\bar{1},\bar{3},\bar{4}}^{+++} \right)^* \quad (181)$$

$$I_{d1,2,3,4}^{--++} = \left( I_{d\bar{2},\bar{1},\bar{3},\bar{4}}^{++--} \right)^* \quad (182)$$

$$I_{d1,2,3,4}^{+-+-} = \left( I_{d\bar{2},\bar{1},\bar{3},\bar{4}}^{+-+-} \right)^* \quad (183)$$

$$I_{d1,2,3,4}^{-+--} = \left( I_{d\bar{2},\bar{1},\bar{3},\bar{4}}^{-+--} \right)^* \quad (184)$$

Thus, only 8 of them are independent. This 8 coefficients can be chosen as:

$$I_{d1,2,3,4}^{++++} = \frac{\pi \mu_B^2}{2A} \iint dx dx' \times \left[ (q_{1z} + q_{2z})^2 (u_1^* v_2^* + v_1^* u_2^*) (u_3^* v_4^* + v_3^* u_4^*) G_{|\mathbf{q}_1 + \mathbf{q}_2|} (x - x') - u_1^* v_2^* u_3^* u_4^* (d_x + q_{4y})^2 G_{|\mathbf{q}_4|} (x - x') + u_1^* v_2^* u_3^* u_4^* (d_x^2 - q_{4y}^2) G_{|\mathbf{q}_4|} (x - x') + u_1^* v_2^* v_3^* u_4^* (d_x^2 - q_{4y}^2) G_{\mathbf{q}_4} (x - x') - u_1^* v_2^* v_3^* v_4^* (d_x - q_{4y})^2 G_{\mathbf{q}_4} (x - x') \right] \quad (185)$$

$$\begin{aligned}
I_{d1,2,3,4}^{-+++} &= -\frac{\pi\mu_B^2}{2A} \iint dx dx' \times \\
&\left[ (q_{1z} + q_{2z})^2 (v_1 v_2^* + v_1^* v_2) (u_3^* v_4'^* + v_3'^* u_4^*) G_{|\mathbf{q}_1 + \mathbf{q}_2|} (x - x') \right. \\
&\quad - v_1 v_2^* u_3^* u_4'^* (d_x + q_{4y})^2 G_{|\mathbf{q}_4|} (x - x') \\
&\quad + v_1 v_2^* u_3^* v_4'^* (d_x^2 - q_{4y}^2) G_{|\mathbf{q}_4|} (x - x') \\
&\quad + v_1 v_2^* v_3^* u_4'^* (d_x^2 - q_{4y}^2) G_{\mathbf{q}_4} (x - x') \\
&\quad \left. - v_1 v_2^* v_3^* v_4'^* (d_x - q_{4y})^2 G_{\mathbf{q}_4} (x - x') \right]
\end{aligned} \tag{186}$$

$$\begin{aligned}
I_{d1,2,3,4}^{+-++} &= -\frac{\pi\mu_B^2}{2A} \iint dx dx' \times \\
&\left[ (q_{1z} + q_{2z})^2 (u_1^* u_2 + v_1 u_2^*) (u_3^* v_4'^* + v_3'^* u_4^*) G_{|\mathbf{q}_1 + \mathbf{q}_2|} (x - x') \right. \\
&\quad - u_1^* u_2 u_3^* u_4'^* (d_x + q_{4y})^2 G_{|\mathbf{q}_4|} (x - x') \\
&\quad + u_1^* u_2 u_3^* v_4'^* (d_x^2 - q_{4y}^2) G_{|\mathbf{q}_4|} (x - x') \\
&\quad + u_1^* u_2 v_3^* u_4'^* (d_x^2 - q_{4y}^2) G_{\mathbf{q}_4} (x - x') \\
&\quad \left. - u_1^* u_2 v_3^* v_4'^* (d_x - q_{4y})^2 G_{\mathbf{q}_4} (x - x') \right]
\end{aligned} \tag{187}$$

$$\begin{aligned}
I_{d1,2,3,4}^{++-+} &= -\frac{\pi\mu_B^2}{2A} \iint dx dx' \times \\
&\left[ (q_{1z} + q_{2z})^2 (u_1^* v_2^* + v_1^* u_2^*) (v_3^* v_4'^* + v_3'^* v_4^*) G_{|\mathbf{q}_1 + \mathbf{q}_2|} (x - x') \right. \\
&\quad - u_1^* v_2^* v_3^* u_4'^* (d_x + q_{4y})^2 G_{|\mathbf{q}_4|} (x - x') \\
&\quad + u_1^* v_2^* v_3^* v_4'^* (d_x^2 - q_{4y}^2) G_{|\mathbf{q}_4|} (x - x') \\
&\quad + u_1^* v_2^* u_3^* u_4'^* (d_x^2 - q_{4y}^2) G_{\mathbf{q}_4} (x - x') \\
&\quad \left. - u_1^* v_2^* u_3^* v_4'^* (d_x - q_{4y})^2 G_{\mathbf{q}_4} (x - x') \right]
\end{aligned} \tag{188}$$

$$\begin{aligned}
I_{d1,2,3,4}^{+++ -} &= -\frac{\pi\mu_B^2}{2A} \iint dx dx' \times \\
&\left[ (q_{1z} + q_{2z})^2 (u_1^* v_2^* + v_1^* u_2^*) (u_3^* u_4' + u_3' u_4^*) G_{|\mathbf{q}_1 + \mathbf{q}_2|} (x - x') \right. \\
&\quad - u_1^* v_2^* u_3^* v_4' (d_x + q_{4y})^2 G_{|\mathbf{q}_4|} (x - x') \\
&\quad + u_1^* v_2^* u_3^* u_4' (d_x^2 - q_{4y}^2) G_{|\mathbf{q}_4|} (x - x') \\
&\quad + u_1^* v_2^* v_3^* v_4' (d_x^2 - q_{4y}^2) G_{\mathbf{q}_4} (x - x') \\
&\quad \left. - u_1^* v_2^* v_3^* u_4' (d_x - q_{4y})^2 G_{\mathbf{q}_4} (x - x') \right]
\end{aligned} \tag{189}$$

$$\begin{aligned}
I_{d1,2,3,4}^{++--} &= \frac{\pi\mu_B^2}{2A} \iint dx dx' \times \\
&\left[ (q_{1z} + q_{2z})^2 (u_1^* v_2^* + v_1^* u_2^*) (v_3^* u_4' + u_3' v_4^*) G_{|\mathbf{q}_1 + \mathbf{q}_2|} (x - x') \right. \\
&\quad - u_1^* v_2^* v_3^* v_4' (d_x + q_{4y})^2 G_{|\mathbf{q}_4|} (x - x') \\
&\quad + u_1^* v_2^* v_3^* u_4' (d_x^2 - q_{4y}^2) G_{|\mathbf{q}_4|} (x - x') \\
&\quad + u_1^* v_2^* u_3^* v_4' (d_x^2 - q_{4y}^2) G_{\mathbf{q}_4} (x - x') \\
&\quad \left. - u_1^* v_2^* u_3^* u_4' (d_x - q_{4y})^2 G_{\mathbf{q}_4} (x - x') \right]
\end{aligned} \tag{190}$$

$$\begin{aligned}
I_{d1,2,3,4}^{+-+-} &= \frac{\pi\mu_B^2}{2A} \iint dx dx' \times \\
&\left[ (q_{1z} + q_{2z})^2 (u_1^* u_{\bar{2}} + u_{\bar{1}} u_2^*) \left( u_3^* u_{\bar{4}}' + u_{\bar{3}}' u_4^* \right) G_{|\mathbf{q}_1 + \mathbf{q}_2|} (x - x') \right. \\
&\quad - u_1^* u_{\bar{2}} u_3^* v_{\bar{4}}' (d_x + q_{4y})^2 G_{|\mathbf{q}_4|} (x - x') \\
&\quad + u_1^* u_{\bar{2}} u_3^* u_{\bar{4}}' (d_x^2 - q_{4y}^2) G_{|\mathbf{q}_4|} (x - x') \\
&\quad + u_1^* u_{\bar{2}} v_3^* v_{\bar{4}}' (d_x^2 - q_{4y}^2) G_{\mathbf{q}_4} (x - x') \\
&\quad \left. - u_1^* u_{\bar{2}} v_3^* u_{\bar{4}}' (d_x - q_{4y})^2 G_{\mathbf{q}_4} (x - x') \right]
\end{aligned} \tag{191}$$

$$\begin{aligned}
I_{d1,2,3,4}^{-++-} &= \frac{\pi\mu_B^2}{2A} \iint dx dx' \times \\
&\left[ (q_{1z} + q_{2z})^2 (v_{\bar{1}} v_2^* + v_1^* v_{\bar{2}}) \left( v_{\bar{3}}' v_4^* + v_3^* v_{\bar{4}}' \right) G_{|\mathbf{q}_1 + \mathbf{q}_2|} (x - x') \right. \\
&\quad - v_{\bar{1}} v_2^* v_{\bar{3}}' v_4^* (d_x + q_{4y})^2 G_{|\mathbf{q}_4|} (x - x') \\
&\quad + v_{\bar{1}} v_2^* v_{\bar{3}}' v_4^* (d_x^2 - q_{4y}^2) G_{|\mathbf{q}_4|} (x - x') \\
&\quad + v_{\bar{1}} v_2^* u_{\bar{3}}' u_4^* (d_x^2 - q_{4y}^2) G_{\mathbf{q}_4} (x - x') \\
&\quad \left. - v_{\bar{1}} v_2^* u_{\bar{3}}' v_4^* (d_x - q_{4y})^2 G_{\mathbf{q}_4} (x - x') \right]
\end{aligned} \tag{192}$$

All the integrals participating in  $I_d$  can be calculated explicitly since the integrand is the product of sines, cosines and exponential function of  $|x - x'|$ . However, the large number of different combinations of sines and cosines and the necessity to use different exponents depending on the sign of  $x - x'$  makes real calculation sufficiently tiresome to charge a computer with this task. For the coefficients  $I_e$  the calculations are much simpler since they include only sines and cosines and integrals over one variable  $x$ . However, 6 independent coefficients  $I_e$  contain about 30 different integrals, so that charging computer with this task is again justified.

### Appendix 3. $1/|\mathbf{r}-\mathbf{r}'|$ -identity .

From the Fourier transformation of  $\frac{1}{|\mathbf{r}-\mathbf{r}'|}$  we have

$$\begin{aligned}
\frac{1}{|\mathbf{r} - \mathbf{r}'|} &= \frac{1}{(2\pi)^3} \iiint_{-\infty}^{\infty} d\mathbf{q} e^{i\mathbf{q}\mathbf{r}} \frac{4\pi}{q^2} \\
&= \frac{1}{(2\pi)^3} \iiint_{-\infty}^{\infty} d\mathbf{q} e^{i\mathbf{q}_{\parallel}(\mathbf{r}_{\parallel} - \mathbf{r}'_{\parallel}) + iq_x(x - x')} \frac{4\pi}{q_{\parallel}^2 + q_x^2} \\
&= \frac{1}{(2\pi)^3} \iint_{-\infty}^{\infty} dq_y dq_z e^{i\mathbf{q}_{\parallel}(\mathbf{r}_{\parallel} - \mathbf{r}'_{\parallel})} \int_{-\infty}^{\infty} dq_x e^{iq_x(x - x')} \frac{4\pi}{q_{\parallel}^2 + q_x^2}
\end{aligned}$$

Since  $\int_{-\infty}^{\infty} dq_x e^{iq_x(x-x')} \frac{4\pi}{q_{\parallel}^2+q_x^2} = \frac{4\pi^2}{q_{\parallel}} e^{-q_{\parallel}|x-x'|} = 8\pi^2 G_{q_{\parallel}}$  Then we get the 1/r-G-identity

$$\frac{1}{|\mathbf{r}-\mathbf{r}'|} = \frac{1}{\pi} \iint_{-\infty}^{\infty} dq_y dq_z e^{i\mathbf{q}_{\parallel}(\mathbf{r}_{\parallel}-\mathbf{r}'_{\parallel})} G_{q_{\parallel}}(x-x') \quad (193)$$

## References

- [1] L.D. Landau and E.M. Lifshitz, Phys. Zs. Sowiet. **8**, 153, 1935.
- [2] L.D. Landau and E.M. Lifshitz, Electrodynamics of Continuous Media, Elsevier, 2nd Edition, 1984, Ch. 5.
- [3] E. Schlöman, Phys. Rev. **116**, 828 (1959).
- [4] Pavol Krivosik and Carl E. Patton, Phys. Rev. B **82**, 184428 (2010).
- [5] R.W. Damon and J.R. Eshbach, J. Phys. Chem. Solids **19**, 308 (1961).
- [6] V.V. Gann, Sov. Phys. Solid State **8**, 2537.
- [7] T. Wolfram and R.R. De Wames, Phys. Rev. Lett. **24**, 1489 (1970).
- [8] B.A. Kalinikos, IEEE Proc. H **127**, 4 (1980).
- [9] B.A. Kalinikos and A.N. Slavin, J. Solid State Phys. **19**, 7013 (1986).
- [10] R.E. Arias, Phys. Rev. B **94**, 134408 (2016).
- [11] Gang.Li, Chen Sun, T. Nattermann and V.L. Pokrovsky, Phys. Rev. B **98**, 014436 (2018).
- [12] S.O. Demokritov, V.E. Demidov, O. Dzyapko, G.A. Melkov, A.A. Serga, B. Hillebrands, and A.N. Slavin, Nature (London) **443**, 430 (2006)
- [13] H. Goldstein, C.P. Poole and J. Safko, Classical Mechanics, 3d edition, Pearson Education, 2011.
- [14] I.V. Kolokolov, V.S. L'vov and V.B. Cherepanov, Zh. Eksp. Theor. Fiz. **84**, 1043 (1983) [Sov. Phys. JETP **57**, 605 (1983).
- [15] E.B. Sonin, Phys. Rev. B **95**, 144432 (2017).
- [16] A. Kreisel, F.Sauli, L. Bartosch, and P. Kopietz, Eur. Phys. J B **71**, 59 (2009).
- [17] A. A. Serga, C. W. Sandweg, V. I. Vasyuchka, M. B. Jungfleisch, B. Hillebrands, A. Kreisel, P. Kopietz, and M. P. Kostylev. Phys. Rev. B **86**, 134403 (2012)

- [18] V. E. Demidov, O. Dzyapko, S. O. Demokritov, G. A. Melkov, and A. N. Slavin, *Phys. Rev. Lett.* **100**, 047205 (2008).
- [19] J. Lim, W. Bang, J. Trossman, A. Kreisel, M.B. Jüngerfleisch, A. Hoffmann, C.S. Tsai and J.B. Ketterson, Study of micron scale dispersion of spin waves in Yttrium Iron Garnet film. Abstract of presentation at March APS Meeting 2018, Los Angeles.
- [20] Chen Sun, Thomas Nattermann and Valery L Pokrovsky, *J. Phys. D: Appl. Phys.* **50**, 143002 (2017).
- [21] Y.M. Bunkov and G.E. Volovik, *J. Low Temp. Phys.* **150**, 135 (2008).
- [22] P. Novik-Boltyk, O. Dzyapko, V.E. Demidov, N.G. Berloff and S.O. Demokritov, *Sci. Rep.* **2**, 482 (2012).
- [23] Fuxiang Li, Wayne M. Saslow, and Valery L. Pokrovsky *Sci Rep* **3**, 1372 (2013)
- [24] C.C. Bradley, C.A. Sackett, and R.G. Hulet, *Phys. Rev. Lett.* **78**, 985, (1997); C.C. Bradley, C.A. Sackett, and R.G. Hulet, *Phys. Rev. A* **55**, 3951, (1997).
- [25] J. L. Roberts, N. R. Claussen, S. L. Cornish, E. A. Donley, E. A. Cornell, and C. E. Wieman *Phys. Rev. Lett.* **86**, 4211 (2001).
- [26] Eric J. Mueller and Gordon Baym, *Phys. Rev. A* **62**, 053605 (2000).
- [27] L.P. Pitaevskii, *Physics Letters A* **221**, 14 (1996).
- [28] Borisenko, I., Divinskiy, B., Demidov, V. *et al.* Direct evidence of spatial stability of Bose-Einstein condensate of magnons. *Nat Commun* **11**, 1691 (2020).
- [29] Borisenko, I.V., Demidov, V.E., Pokrovsky, V.L. *et al.* Spatial separation of degenerate components of magnon Bose-Einstein condensate by using a local acceleration potential. *Sci Rep* **10**, 14881 (2020).
- [30] I. S. Tupitsyn, P. C. E. Stamp, and A. L. Burin. Stability of Bose-Einstein Condensates of Hot Magnons in Yttrium Iron Garnet Films. *Phys. Rev. Lett.* **100**, 257202 (2008).
- [31] S.M. Rezende. Theory of coherence in Bose-Einstein condensation phenomena in a microwave-driven interacting magnon gas. *Phys. Rev. B* **79**, 174411 (2009).
- [32] Divinskiy, B., Merbouche, H., Demidov, V.E. *et al.* Evidence for spin current driven Bose-Einstein condensation of magnons. *Nat Commun* **12**, 6541 (2021).

- [33] Noack, Timo B. and Vasyuchka, Vitaliy I. and Pomyalov, Anna and L'vov, Victor S. and Serga, Alexander A. and Hillebrands, Burkard, Evolution of room-temperature magnon gas: Toward a coherent Bose-Einstein condensate, *Phys. Rev. B* **104**, L100410 (2021).